NUREG/CR-5165

Seismological Investigation of Earthquakes in the New Madrid Seismic Zone and the Northeastern Extent of the New Madrid Seismic Zone

Final Report
September 1981-December 1986

Prepared by R.B. Herrmann, K. Taylor, B. Nguyen

Department of Earth and Atmospheric Sciences
Saint Louis University
St. Louis, MO 63103

Prepared for
U.S. Nuclear Regulatory
Commission

NOTICE

Availability of Reference Materials Cited in NRC Publications

Most documents cited in NRC publications will be available from one of the following sources:

1. The NRC Public Document Room, 1717 H Street, N.W.
   Washington, DC 20555
2. The Superintendent of Documents, U.S. Government Printing Office, Post Office Box 37082, Washington, DC 20013-7082
3. The National Technical Information Service, Springfield, VA 22161

Although the listing that follows represents the majority of documents cited in NRC publications, it is not intended to be exhaustive.

Referenced documents available for inspection and copying for a fee from the NRC Public Document Room include NRC correspondence and internal NRC memoranda; NRC Office of Inspection and Enforcement bulletins, circulars, information notices, inspection and investigation notices; Licensee Event Reports; vendor reports and correspondence; Commission papers; and applicant and licensee documents and correspondence.

The following documents in the NUREG series are available for purchase from the GPO Sales Program: formal NRC staff and contractor reports, NRC-sponsored conference proceedings, and NRC booklets and brochures. Also available are Regulatory Guides, NRC regulations in the *Code of Federal Regulations*, and *Nuclear Regulatory Commission Issuances*.

Documents available from the National Technical Information Service include NUREG series reports and technical reports prepared by other federal agencies and reports prepared by the Atomic Energy Commission, forerunner agency to the Nuclear Regulatory Commission.

Documents available from public and special technical libraries include all open literature items, such as books, journal and periodical articles, and transactions. *Federal Register* notices, federal and state legislation, and congressional reports can usually be obtained from these libraries.

Documents such as theses, dissertations, foreign reports and translations, and non-NRC conference proceedings are available for purchase from the organization sponsoring the publication cited.

Single copies of NRC draft reports are available free, to the extent of supply, upon written request to the Division of Information Support Services, Distribution Section, U.S. Nuclear Regulatory Commission, Washington, DC 20555.

Copies of industry codes and standards used in a substantive manner in the NRC regulatory process are maintained at the NRC Library, 7920 Norfolk Avenue, Bethesda, Maryland, and are available there for reference use by the public. Codes and standards are usually copyrighted and may be purchased from the originating organization or, if they are American National Standards, from the American National Standards Institute, 1430 Broadway, New York, NY 10018.

NUREG/CR-5165
RA

Seismological Investigation of Earthquakes in the New Madrid Seismic Zone and the Northeastern Extent of the New Madrid Seismic Zone

Final Report
September 1981-December 1986

Manuscript Completed: May 1988
Date Published: July 1988

Prepared by
R.B. Herrmann, K. Taylor, B. Nguyen

Department of Earth and Atmospheric Sciences
Saint Louis University
St. Louis, MO 63103

Prepared for
Division of Engineering
Office of Nuclear Regulatory Research
U.S. Nuclear Regulatory Commission
Washington, DC 20555
NRC FIN D1694
Under Contract No. NRC-04-81-195-03

Abstract

Earthquake activity in the Central Mississippi Valley has been monitored by an eight station seismograph network in the Wabash River Valley of southeastern Illinois and by a six station seismograph network in the New Madrid seismic zone. This network is a major component of a larger network in the region, jointly sponsored by the NRC, USGS, universities and states.

During the time period of the contract, October 1981 through December 1986, 1206 earthquakes were located in the Central Mississippi Valley, of which 808 were in the New Madrid, Missouri area. Significant earthquakes studied in detail occurred in northeastern Ohio on January 31, 1986 and in southeastern Illinois on June 10, 1987.

Focal mechanisms have been calculated for the 10 June 1987 southern Illinois earthquake using both P-wave first motions and long-period surface-wave spectral amplitude data. Using 225 long-period Rayleigh-wave and 113 long-period Love-wave spectral amplitude-period data points, a systematic search was performed to find the focal depth, focal mechanism and seismic moment which best described the observed radiation pattern. The solution which best fit the surface wave data together with the P-wave first motion data is one with a focal depth of 10 ± 1 km, a seismic moment of $3.1 \, x \, 10^{23}$ dyne-cm, and a focal mechanism characterized by a pressure axis that trends 89° and plunges 4° and a tension axis that trends 357° and plunges 24°.

The long-period surface-wave and strong ground motion accelerogram recordings of the January 31, 1986 northeastern Ohio earthquake were used to estimate the focal mechanism and source time function of the source. The surface-wave solution requires a source with a depth of 7 km, a seismic moment of $1.1 \, x \, 10^{23}$ $dyne-cm$, and a focal mechanism characterized by a pressure axis that trends 336° and plunges 21° and a tension axis that trends 70° and plunges 7°. Attempts at modeling the observed strong motion accelerogram are hampered by lack of knowledge of the exact earth model, but the surface-wave focal mechanism, source depth and seismic moment are adequate if the total duration of the source time function is about 0.3-0.4 seconds.

Table of Contents

List of Figures

List of Tables

INTRODUCTION

This report summarizes the results of operating a regional seismic network for the U. S. Nuclear Regulatory Commission under Contract No. NRC 04-81-195-03, for the time period between September 29, 1981 and December 31, 1986. Since most of the work performed has been published in theses, journals and in the quarterly seismic bulletin, this report provides a summary of findings as well as two short sections on recent large earthquakes of interest.

SEISMIC NETWORK RESULTS

The NRC seismic network is a component of a larger regional network operated by Saint Louis University, Memphis State University, the University of Kentucky, the University of Michigan and other groups. Figure 1 presents a map of the central United States centered about New Madrid, Missouri. The seismograph station locations are indicated by the triangles with station codes printed adjacent to them. The NRC sponsored stations of Saint Louis University occupy two regions. The stations SPIN, WSIL, WDIN, NHIL, CIRL, BPIL, CSIL and GOIL provide coverage in the Wabash River Valley, while the stations ACTN, BBTN, OGTN, SJMO, ACMO and WGAR provided complementary coverage to the USGS stations in the New Madrid Region. The locations of these stations are listed in Table 1 and are plotted on Figure 1.

The network consists of sensors in the field, whose signals are transmitted to St. Louis by a combination of radio and telephone links. At St. Louis, the signals are recorded on analog media, 16mm photographic film and pen and ink recorders, as well as by a digital computer. In addition to the stations run by Saint Louis University, selected stations of Memphis State University are digitized and archived for future research.

Network operational status, seismic phase readings and earthquake locations are presented in the quarterly publication, *Central Mississippi Valley Earthquake Bulletin*, published by Saint Louis University. This bulletin consists of readings of earthquakes located by the Saint Louis University network and additional readings from cooperating institutions to yield as complete an archive source as possible for the region. During the time period of this contract, Bulletins 30 - 50 were compiled and distributed to over 100 organizations.

Seismicity

Figure 2 presents a map showing the locations of 1206 earthquakes located in the time period 1 October 1981 - 31 December 1986. This map encompasses the New Madrid Seismic Zone at the center, the seismicity in the Wabash River Valley, and the southern extent of the New Madrid Seismic Zone monitored by Memphis State University. The symbol sizes on this map are keyed to the earthquake size. The bulk of the seismicity occurs near New Madrid. Other, interesting trends are slowly developing with continued monitoring. For example, there is a diffuse trend 100 km west of and sub-parallel to the main New Madrid trend. This trend extends from Cape Girardeau, MO (CGM) southwest to Olyphant, TN (OLY). The extensive Arkansas earthquake swarm started in January, 1981 and was located just west of OLY. Another set of short trends occurs in southern Illinois near the confluence of the Ohio and Mississippi Rivers. One of these trends is between the stations GOIL and WCK, and the other is about 20 km northwest. Again we note that these patterns trend in a northeast-southwest direction. The activity in the Wabash River Valley is at a lower level, even though several magnitude 3+ earthquakes occurred during this time period, and a magnitude 5+ occurred in June, 1987.

Figure 3 presents the same earthquake locations, but with a symbol size keyed to earthquake focal depth. Earthquake focal depth is not an easy parameter to determine. Arrival time data are required at distances less than two source depths, or at a large range of distances so that the subtle effect of depth on the travel time curves can be used. The earthquakes in the Wabash Valley are interesting because many have well located depths at depths greater than 15 km, some in the 20 - 25 km range. This is interesting because the typical New Madrid event has depths less than 15 km; The ones disagreeing with this assessment are rare, and could be attributed to poor location/depth control. The large number of deeper events in the Ozark Uplift, near the WWSSN station FVM, may be real, or may be a systematic artifact of poor network control.

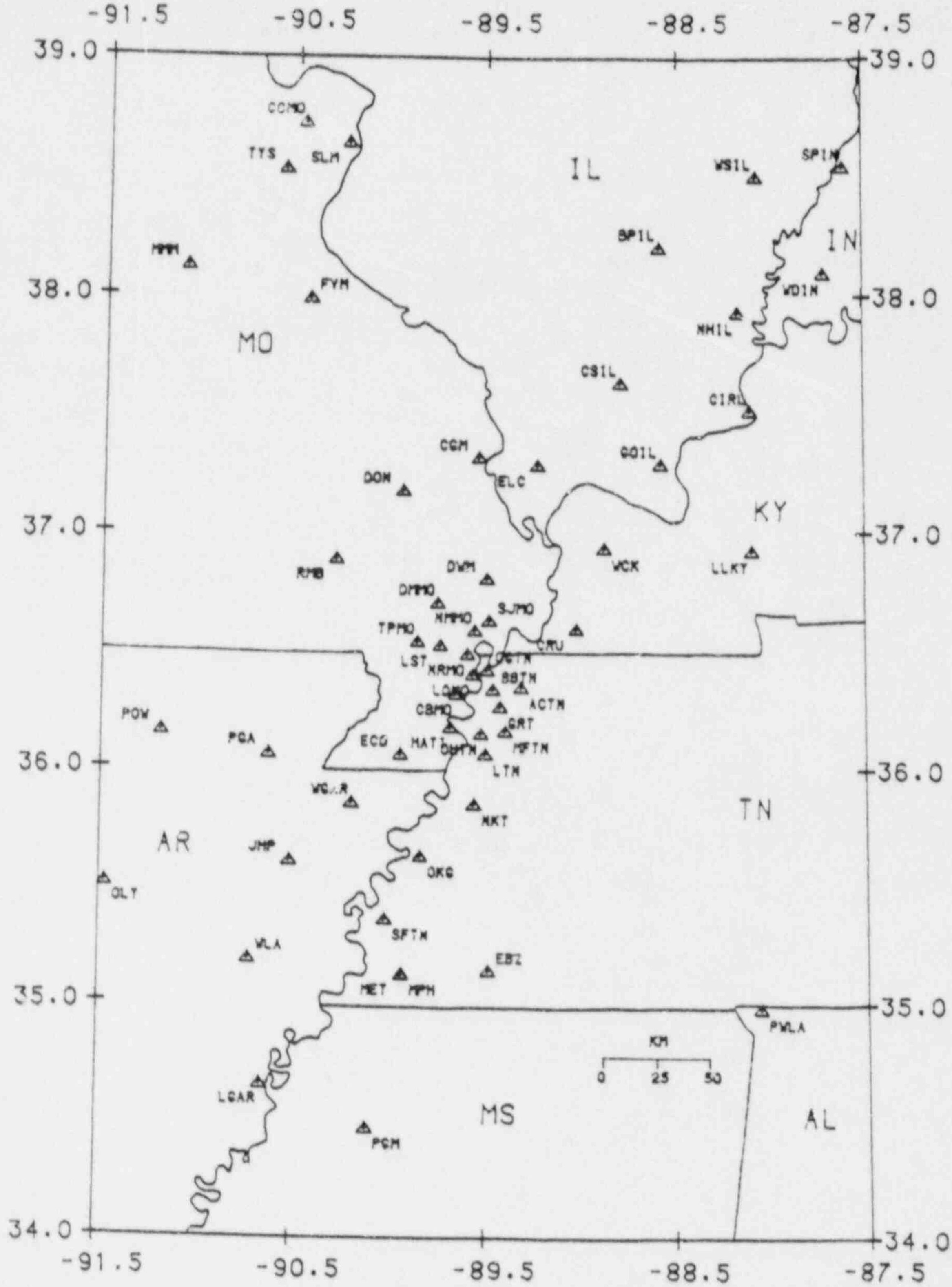

Fig. 1. Location of seismograph stations monitoring earthquakes in the Central Mississipi Valley.

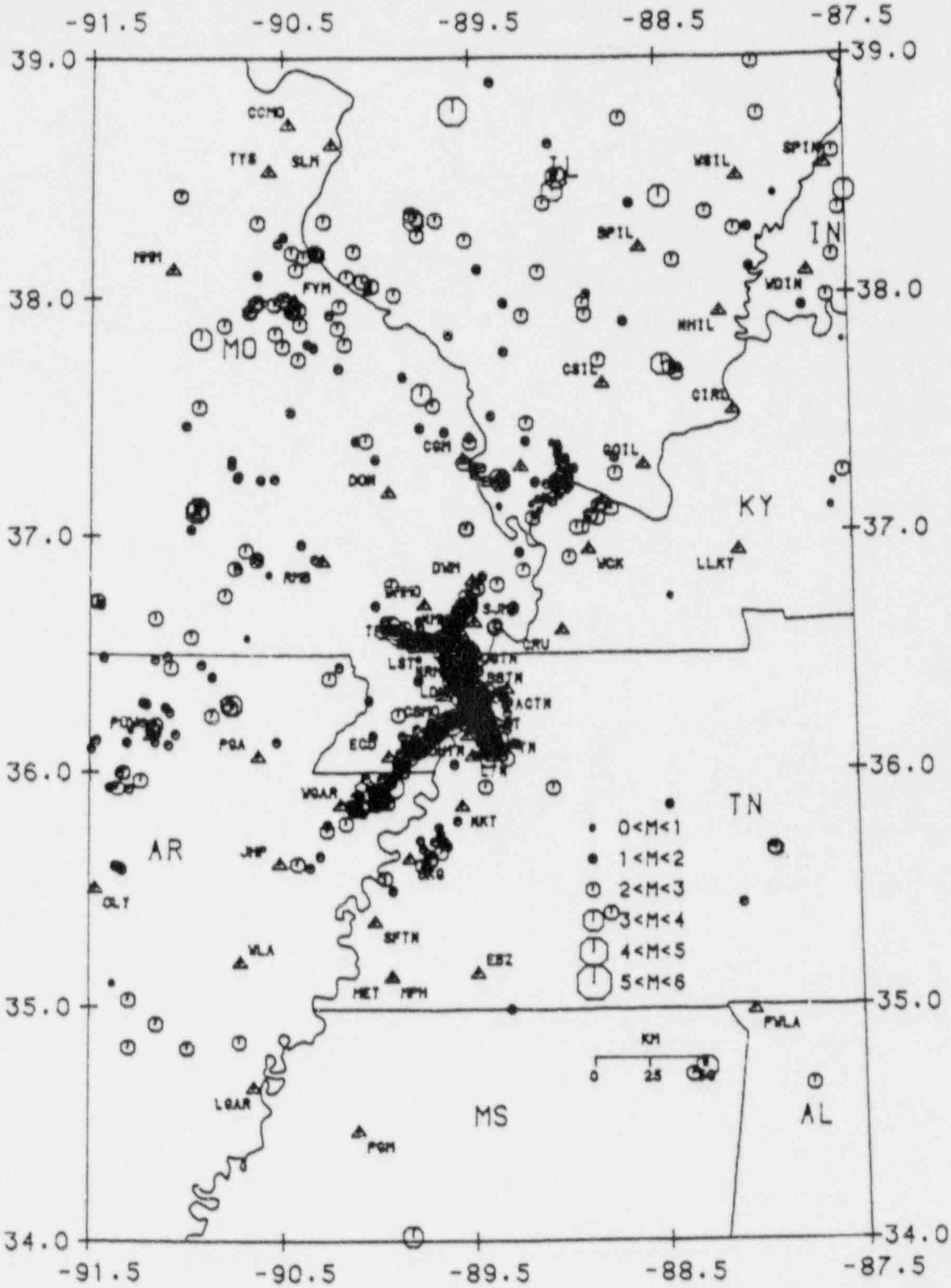

Fig. 2. Earthquakes located between 1 October 1981 and 31 December 1986. The symbol sizes are keyed to the earthquake magnitude.

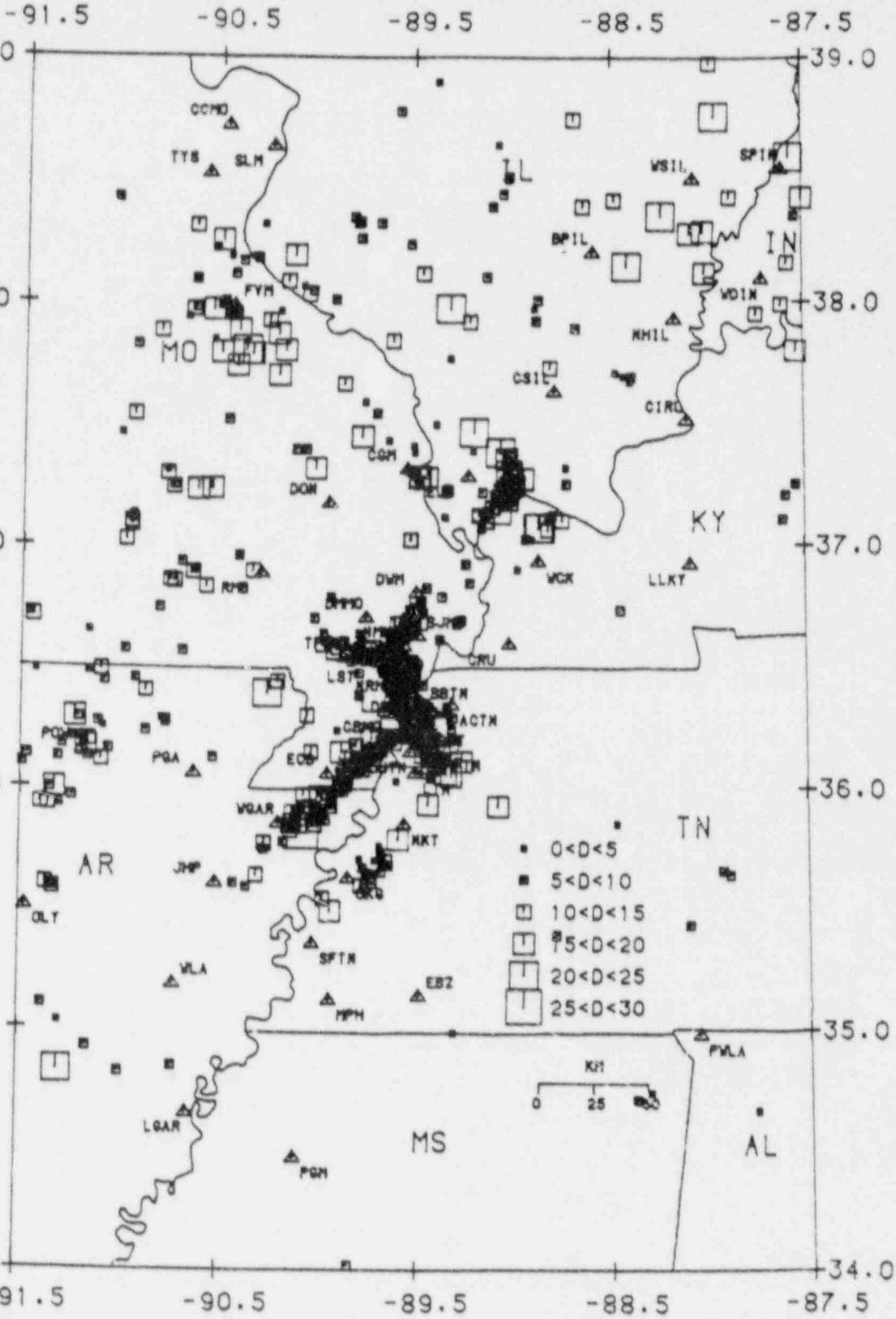

Fig. 3. Earthquakes located between 1 October 1981 and 31 December 1986. The symbols are keyed to the earthquake depth.

Focusing more on the New Madrid Seismic Zone, Figure 4 shows the locations of 808 earthquakes with symbols keyed on magnitude. Figure 5 shows the same region with the symbol keyed on focal depth. Many small events are located, with very well defined trends. One major feature is a 115 km northeast striking trend from northeastern Arkansas through the Missouri Bootheel into Tennessee. Here a dense, diffuse 60 km long pattern trends in a southeast-northwest direction. At the northwest end, other narrow trends splay off to the west and to the northeast.

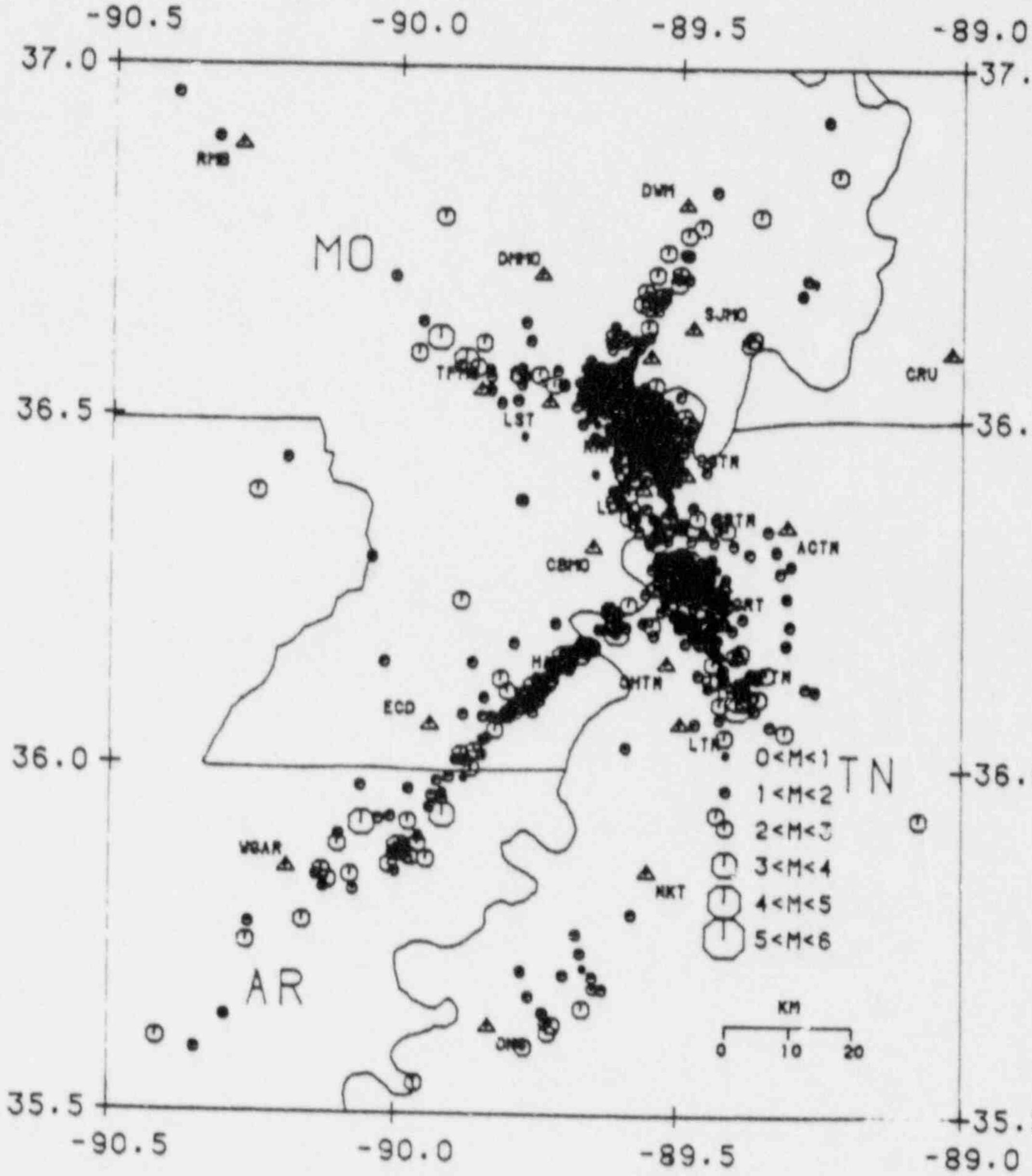

Fig. 4. Earthquakes located between 1 October 1981 and 31 December 1986 in a region near New Madrid, Missouri. The symbols are keyed to the earthquake magnitude.

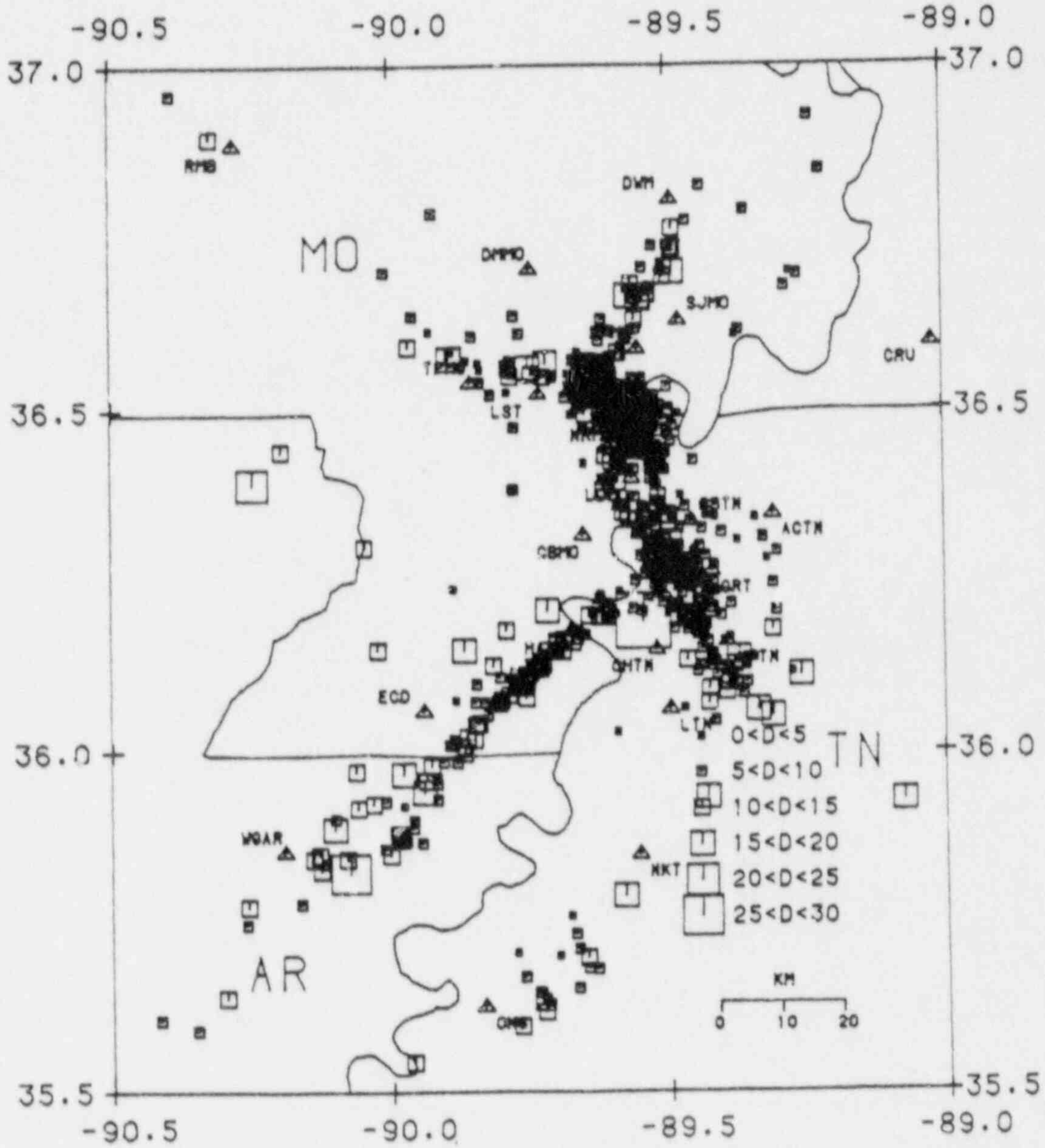

Fig. 5. Earthquakes located between 1 October 1981 and 31 December 1986 in a region near New Madrid, Missouri. The symbols are keyed to the earthquake depth.

TABLE 1

Location of Stations

A. Stations of SLU Seismic Network

	Lat.	Long.	Elevation (meters)
NRC Stations			
BPIL Belle Prairie, IL	38.202N	88.592W	113
CIRL Cave In Rock, IL	37.513N	88.107W	119
CSIL Creal Springs, IL	37.632N	88.790W	168
GOIL Rosebud, IL	37.290N	88.580W	88
NHIL New Haven, IL	37.927N	88.171W	134
SJMO St. John's Bayou, MO	36.629N	89.476W	91
SPIN Swan Pond Ditch, IN	38.540N	87.607W	122
WDIN Wadesville, IN	38.091N	87.716W	164
WGAR Walnut Grove, AR	35.853N	90.191W	72
WSIL West Salem, IL	38.498N	88.075W	155
ACTN Antioch Church, TN	36.347N	89.310W	143
BBTN Blue Bank Bayou, TN	36.387N	89.457W	88
OGTN Old Graveyard Slough, TN	36.420N	89.486W	91
ACMO Noranda, MO	36.487N	89.588W	88
USGS Stations			
CBMO Cypress Bend, MO	36.317N	89.651W	84
CCMO Creve Couer, MO	38.720N	90.467W	152
CRU Crutchfield, KY	36.595N	89.020W	127
DMMO Demmitville, MO	36.704N	89.745W	89
DON Dongola, MO	37.176N	89.933W	165
DWM Dogwood, MO	36.805N	89.490W	92
ECD Elk Chute Ditch, MO	36.060N	89.940W	79
ELC Elco, IL	37.285N	89.227W	153
FVM French Village, MO	37.984N	90.426W	334
GOIL Rosebud, IL	37.290N	88.580W	165
GRT Gratio, TN	36.264N	89.420W	137
HATI Hayti, MO	36.177N	89.676W	83
JHP Judd Hill Pltn., AR	35.605N	90.510W	68
LDMO Linda, MO	36.411N	89.563W	86
LST Lone Star, MO	36.523N	89.731W	83
LTN Lennox, TN	36.063N	89.495W	146
NKT Nankipoo, TN	35.850N	89.554W	153
NMMO New Madrid, MO	36.588N	89.552W	90
NRMO Noranda, MO	36.487N	89.588W	88
OKG Oak Grove, TN	35.626N	89.835W	129
PGA Paragould, AR	36.060N	90.620W	122
POW Powhatan, AT	36.152N	91.185W	156
RMB Rombauer, MO	36.886N	90.278W	147
SLM St. Louis, MO	38.636N	90.236W	161
TPMO Tallapoosa, MO	36.540N	89.852W	83
TYS Tyson Valley, MO	38.527N	90.566W	195

WCK Wilson Creek, KY	36.934N	88.874W	137

B. Other Cooperative Stations

CGM Cape Girardeau, MO	37.317N	89.533W	134
BLO Bloomington, IN	39.172N	86.522W	230

C. Tennessee Earthquake Information Center

MET Memphis, TN (MSU)	35.122N	89.934W	93
MPH Memphis, TN (TEIC)	35.123N	89.932W	94
SFTN Shelby Forest, TN	35.358N	90.019W	-23
WLA Wittsburg Lake, AR	35.186N	90.716W	113
LGAR La Grange, AR	34.651N	90.658W	100
PGM Pleasant Grove, MS	34.464N	90.113W	105
OLY Olyphant, AR	35.503N	91.470W	236
PWLA Pickwick Lake, AL	34.980N	88.064W	204
EBZ Ebenezer, TN	35.141N	89.351W	169
STAR Star City, AR	33.892N	91.778W	107

D. Kansas Geological Survey

BEK Belvue, KS	39.263N	96.200W	349
LAK Lawrence, KS	39.046N	95.204W	260
HWK Hiawatha, KS	39.802N	95.496W	320
EDK El Dorado, KS	37.774N	96.795W	418
EMK Emporia, KS	38.446N	96.317W	370
MLK Milford, KS	39.106N	96.892W	386
TCK Tuttle Creek, KS	39.385N	96.723W	376
SNK Salina, KS	38.953N	97.603W	407
CNK Concordia, KS	39.508N	97.713W	465
JHN Johnson, NE	40.447N	96.019W	329
BENE	40.217N	96.603W	
PCNE	41.539N	97.427W	
LCNE	41.308N	98.939W	
CCNE	40.504N	97.937W	
WHNE	41.236N	96.652W	

E. University of Kentucky

L6KY Lock 6, KY	37.926N	84.820W	
BHKY Bowman Hall, KY	38.035N	84.505W	
SBKY Sharpsburg, KY	38.225N	83.927W	
HEKY Henderson, KY	37.796N	87.652W	
LLKY Land Between the Lakes, KY	36.922N	88.097W	
PKKY Potato Knob, KY	38.383N	83.034W	
SMKY Sacramento, KY	37.423N	87.276W	
SOKY Sonora, KY	37.526N	85.965W	

F. Oklahoma Geophysical Observatory

TUL Leonard, OK	35.911N	95.793W	256
RLO Rose Lookout Tower, OK	36.167N	95.025W	363
SIO Slick, OK	35.746N	97.307W	320

VVO Vivian, OK	35.337N	95.737W	224
ACO Alabaster Caverns, OK	36.699N	99.146W	521
BHO Bethel, OK	34.381N	94.867W	143
WLO Wilson, OK	34.065N	97.369W	284
PCO Ponca City, OK	36.693N	96.982W	324
RRO Red Rock Canyon, OK	35.457N	98.358W	482
QZO Quartz Mountain, OK	34.905N	99.305W	488
OCO Oklahoma City, OK	35.524N	97.474W	351
MEO Meers, OK	34.783N	98.585W	458

G. University of Michigan

AAM Ann Arbor, Mich	42.300N	83.656W	817
ACM	42.647N	85.852W	880
AN1 Anna, Ohio	40.479N	84.131W	1003
AN3	40.549N	83.812W	1070
AN4	40.222N	83.898W	1134
AN7	40.824N	83.860W	922
AN8	40.244N	84.286W	992
AN9	40.712N	84.497W	835
AN10	40.473N	84.470W	901
AN11	40.564N	84.680W	895
AN12	40.922N	84.182W	741
IN1 Indiana	40.542N	85.894W	837
IN2	39.939N	86.783W	872
IN3	39.265N	85.785W	722
IN4	39.570N	84.903W	1025

THESES AND PUBLICATIONS

Although the primary purpose of operating the USNRC network was to define patterns of seismicity that would assist in the correct assessment of seismic hazard, substantial work was performed on the larger problem of earthquakes in the eastern U. S., e.g., earthquake quantification, ground motion characteristics, historical seismicity, etc. The following list of theses and publication reflects this wider interest, and also a perceived obligation to the USNRC to address these topics in addition to the main objective of understanding the regional seismicity.

Theses

Chulick, J. A. (1985). A comparison of M_L to m_{Lg} for large California earthquakes with scaling considerations for strong ground motion, M. S. Thesis, Saint Louis University.

Gordon, D. W. (1983). Revised hypocenters and correlation of seismicity and tectonics in the Central United States, Ph. D. Dissertation, Saint Louis University.

Himes, L. D. (1987). A joint hypocenter velocity determination for the New Madrid Seismic Zone, M. S. Thesis, Saint Louis University.

Leu, P.-L. (1985). Magnitude corrections for the central Mississippi Valley seismic network, M. S. Thesis, Saint Louis University.

Lydon, M. T. (1985). Lg source parameter estimates in various earth models, M. S. Thesis, Saint Louis University.

Nguyen, B. V. (1985). Surface-wave focal mechanisms, magnitudes and energies for some eastern North American earthquakes with tectonic implication, M. S. Thesis, Saint Louis University.

Shin, T.-C. (1985). Lg and coda wave studies of eastern Canada, Ph. D. Dissertation, Saint Louis University.

Publications

Peters, K. and R. B. Herrmann (compilers)(1986). *A collection of historical documents pertaining to the 1886 Charleston, South Carolina earthquake*, Bulletin 41, South Carolina Geological Survey, 116pp.

Herrmann, R. B. and O. W. Nuttli (1982). Magnitude: The relation of M_L to m_{bLg}, *Bull. Seism. Soc. Am.* **72,** 389-397.

Herrmann, R. B., C. A. Langston and J. E. Zollweg (1982). The Sharpsburg, Kentucky earthquake of July 27, 1980, *Bull Seism. Soc. Am.* **72,** 1219-1239.

Herrmann, R. B. (1982). Digital processing of regional network data, *Bull. Seism. Soc. Am.* **72,** S377-S392.

Herrmann, R. B. and A. Kijko (1983). Modeling some empirical Lg relations, *Bull. Seism. Soc. Am.* **73,** 157-171.

Herrmann, R. B. (1982). The relevance of regional networks for the siting of critical facilities, *Earthquake Notes* **53,** 37-48.

Nuttli, O. W. and R. B. Herrmann (1982). Earthquake magnitude scales, *J. Geotech. Engineering Div., Proc. A. S. C. E.*, **108,** 783-786.

Herrmann, R. B. and A. Kijko (1983). Short period Lg magnitudes: Instrument, attenuation and source effects, *Bull. Seism. Soc. Am.* **73,** 1835-1850.

Central Mississippi Valley earthquakes - 1980 (with W. Stauder, S. Singh, R. Perry, R. Dwyer, M. Meremonte, V. Masih, L. Himes, E. Haug, S. Morrissey, L. Hausmann and M. Whittington), 1982. *Earthquake Notes* **53,** 53-56.

Nuttli, O. W. and R. B. Herrmann (1983). Ground Motion of Mississippi Valley Earthquakes, *J. Technical Topics in Civil engineering, A. S. C. E.* **110,** 54-69.

Herrmann, R. B. (1985). An extension of random vibration theory estimates of strong ground motion to large distances, *Bull. Seism. Soc. Am.* **75,** 1447-1453.

Saikia, C. K. and R. B. Herrmann (1985). Application of waveform modeling to determine focal mechanisms of four 1982 Miramichi aftershocks, *Bull. Seism. Soc. Am.* **75,** 1021-1040.

Shin, T.-C. and R. B. Herrmann (1987). Lg attenuation and source studies using 1982 Miramichi data, *Bull. Seism. Soc. Am.* **77,** 384-397.

Herrmann, R. B. (1986). Surface-wave studies of some South Carolina earthquakes, *Bull. Seism. Soc. Am.* **76,** 111,121.

Saikia, C. K. and R. B. Herrmann (1986). Moment-tensor solutions for three 1982 Arkansas swarm earthquakes by waveform modeling, *Bull. Seism. Soc. Am.* **76,** 709-723.

Saikia, C. K. and R. B. Herrmann (1987). Determination of focal mechanisms of some earthquakes at Monticello, South Carolina, and earth structure by waveform modeling, *Geophys. J.* **90**, 669-691.

Chulick, J. A. and R. B. Herrmann (1986). The relation of m_{Lg} to M_L for California earthquakes: observations and modeling, *Earthquake Notes* **57,** 95-102.

Nuttli, O. W., G. A. Bollinger and R. B. Herrmann (1986). The 1886 Charleston, South Carolina, Earthquake - A 1986 Perspective, U. S. Geological Survey Circular 985, 52 pp.

Burger, R. W., P. G. Somerville, J. S. Barker, R. B. Herrmann and D. V. Helmberger (1987). The effect of crustal structure on strong ground motion attenuation relations in eastern North America, *Bull. Seism. Soc. Am.* **77,** 420-439.

Herrmann, R. B. (1987). Broadband Lg magnitude, *Seismological Research Letters* **58,** 125-133.

SOURCE PARAMETERS OF THE SOUTHERN ILLINOIS EARTHQUAKE OF 10 JUNE 1987

By Kenneth B. Taylor and Robert B. Herrmann

Seismic Environment of the Source Region

The magnitude 4.9 m_b (PDE) southern Illinois earthquake of 10 June 1987 was the largest event to occur in the Wabash Valley Seismic Zone since the 5.5 m_b earthquake on 9 November 1968. Using regional seismic network data, the epicenter was located at 38.71 ° N, 87.95 ° W, and had a poorly constrained focal depth of 4.6 km (Stauder *et al.*, 1987). The nearest permanent seismograph station was 30 km southwest of the event. Using data from 12 short-periods vertical records from WWSSN and Canadian Network stations, a trimmed mean magnitude, m_{bLg} = 5.2 was calculated for this earthquake.

The June 10, 1987 earthquake occurred in the Wabash River Valley of southern Illinois. This region is noted for its high level of seismicity, and as such is usually defined to be a source zone is hazard analysis (Barstow *et al*, 1981). During the past 30 years, the two largest earthquakes in the mid-continent occurred here, rather than in the more active New Madrid Seismic Zone to the southwest. Figure 6 provides the locations of earthquakes large enough to be felt for the time period of 1800 - 1974. The map symbol sizes are proportional to magnitude, with the largest symbol corresponding to a magnitude 5.5 earthquake and the smallest to a magnitude 3.5. The historical seismicity has no apparent trends because of the poor locations of many events of the nineteenth century

In July, 1974, a regional seismic network was installed to monitor seismicity in the New Madrid Seismic Zone, which lies off the bottom of Figure 6. Additional stations were provided by the USNRC to provide coverage in the Wabash Valley. Figure 7 shows the locations of 223 earthquakes located from July, 1974 through June, 1987. The dense number of events at 38.71 ° N and 87.95 ° W are aftershocks of the June 10, 1987 event. The pattern of recent seismicity is vaguely similar to the historical pattern of Figure 6. One definite similarity is the tendency for earthquakes to occur in southeastern Illinois subparallel to the Wabash Valley and 25 km to the northwest.

Because of the level of mining activity in the region, there is a possibility of poorly located or non-earthquake events in the catalog. To account for this possibility, Figure 8 presents 96 events for the 1974 - 1987 time period which had free depth locations. Figure 9 shows the locations with symbol sizes keyed to depth. Several intriguing features are apparent. A group of shallow events lies along a narrow northwest - southeast trending belt in southwestern Illinois. This belt is parallel to and 20 km northeast of the geological outcropping associated with surface coal mining. There is a possibility that this trend is associated with underground mining, either as explosions or as seismic activity induced by the material failures in the mines. The earthquakes in the Wabash Valley proper, are distinguished by magnitudes typically greater than 3.0 and depths as deep as 25 km. Scanning the depths of well located earthquakes, over 14 are found with depths in the range of 14 - 25 km. This is a very interesting observation since very few earthquakes in the New Madrid Seismic Zone have depths greater than 14 km, while the Wabash Valley zone has a very large proportion. The paucity of events smaller than magnitude 3 may be a reflection of low station gains required by the installation of a seismic network in a active agricultural region.

Focal Mechanism Studies

The focal mechanism was determined by making combined use of P-wave first motion and surface-wave spectral amplitude data.

P-Wave Analysis

P-wave first motion data were used to define the compressional and dilational quadrants of the focal mechanism and also to resolve the 180 ° ambiguity due to the use of surface waves. Sixty-one P-wave first motions were used to calculate a focal mechanism for the main shock. Incident angles were calculated by the computer program FASTHYPO (Herrmann, 1979a) using an

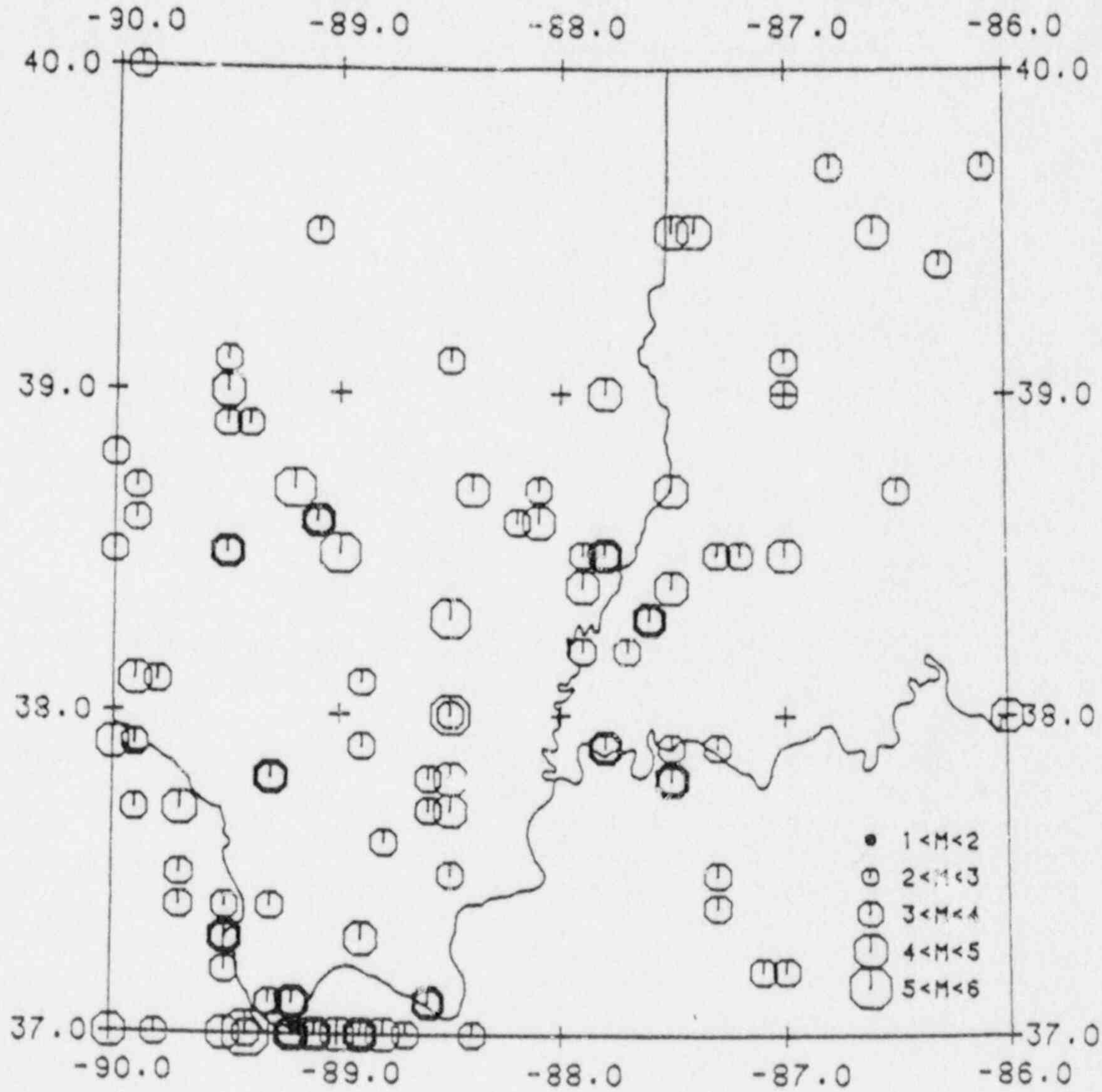

Fig. 6. Historical seismicity in a region centered on the lower Wabash River Valley for the time period 1800 - 1974.

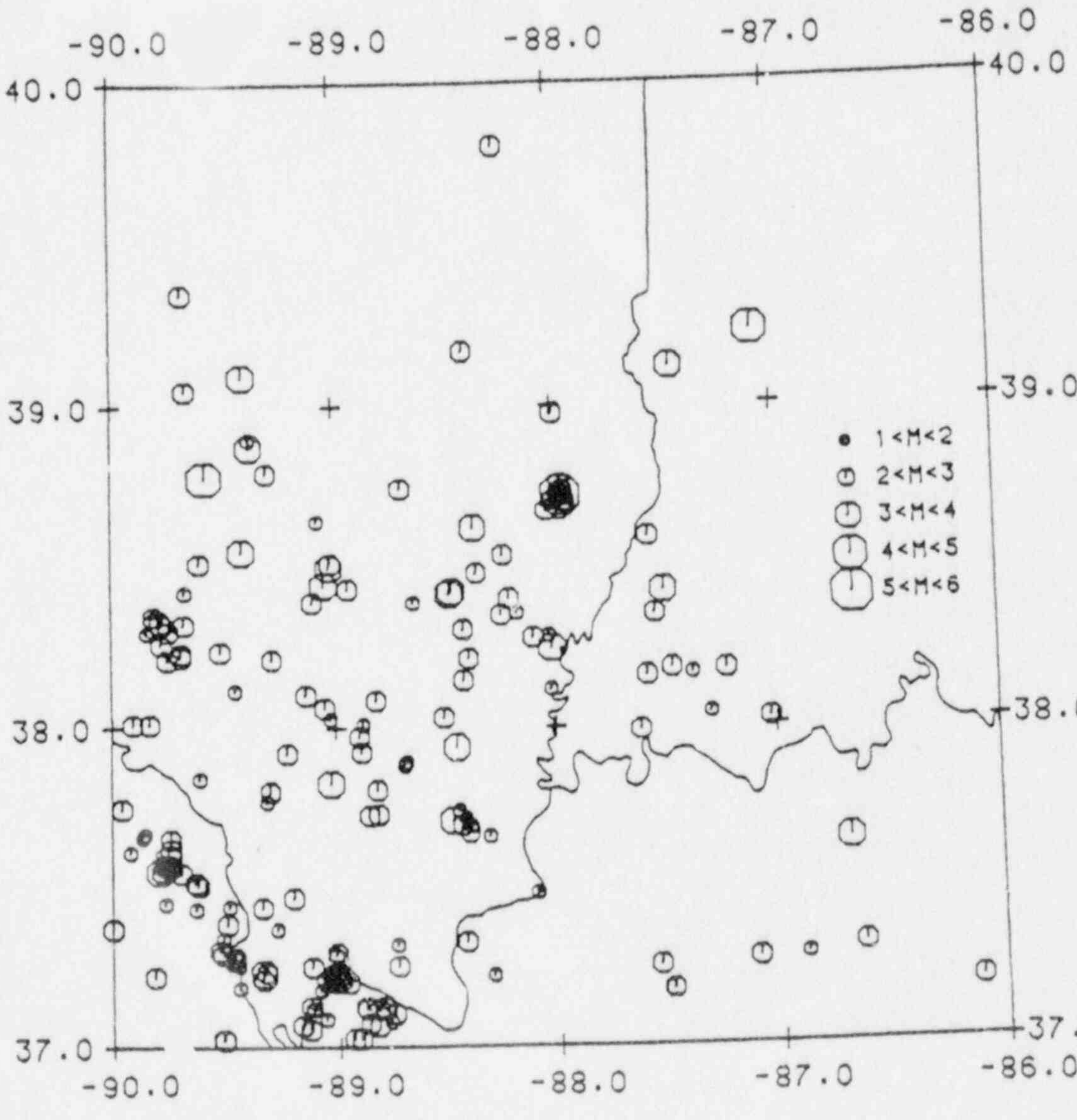

Fig. 7. Instrumental locations for the time period 1974 - 1987. Symbol sizes are keyed to the event magnitude.

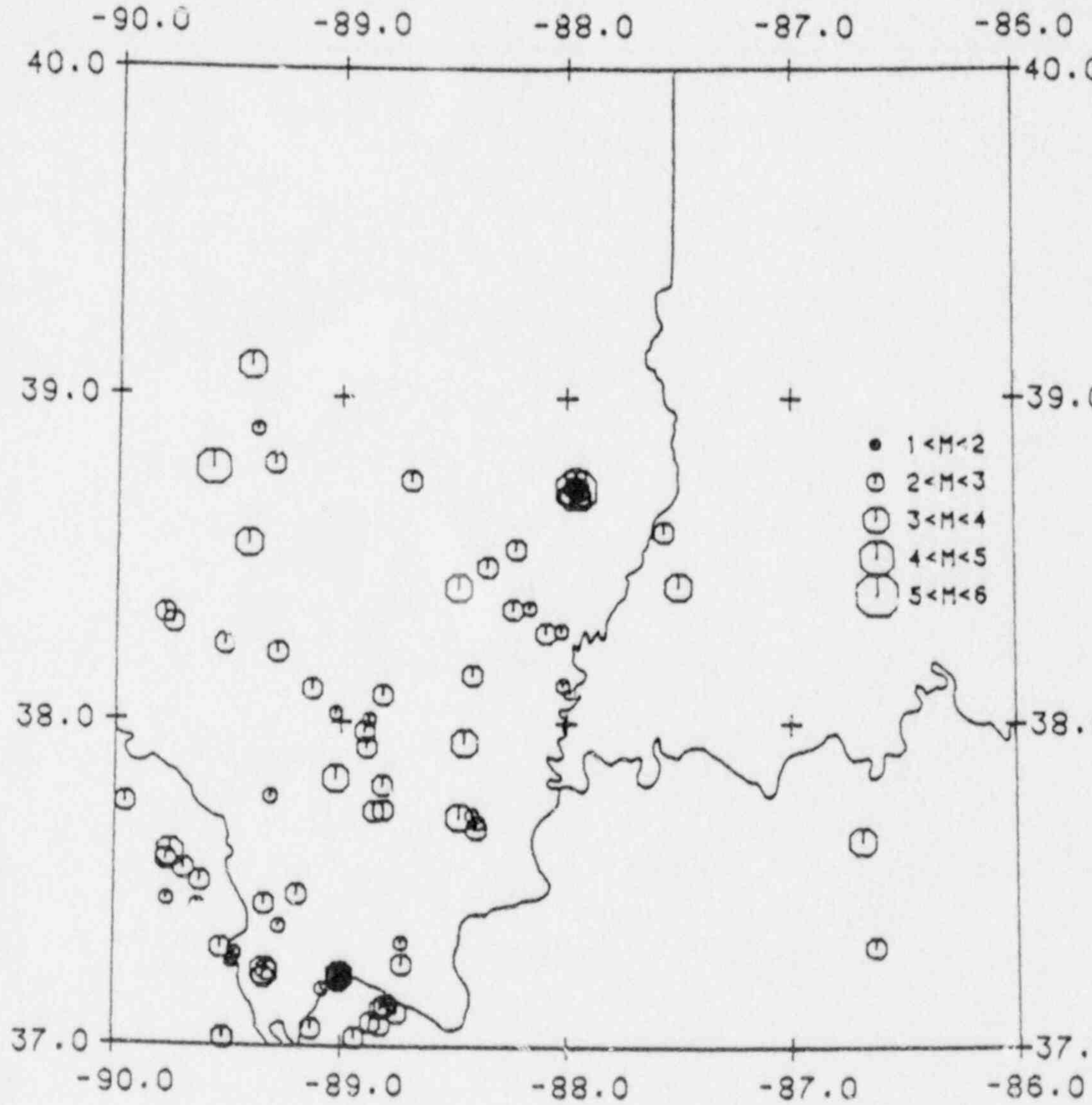

Fig. 8. Free depth instrumental locations for the time period 1974 - 1987. The symbol sizes are keyed to the event magnitude.

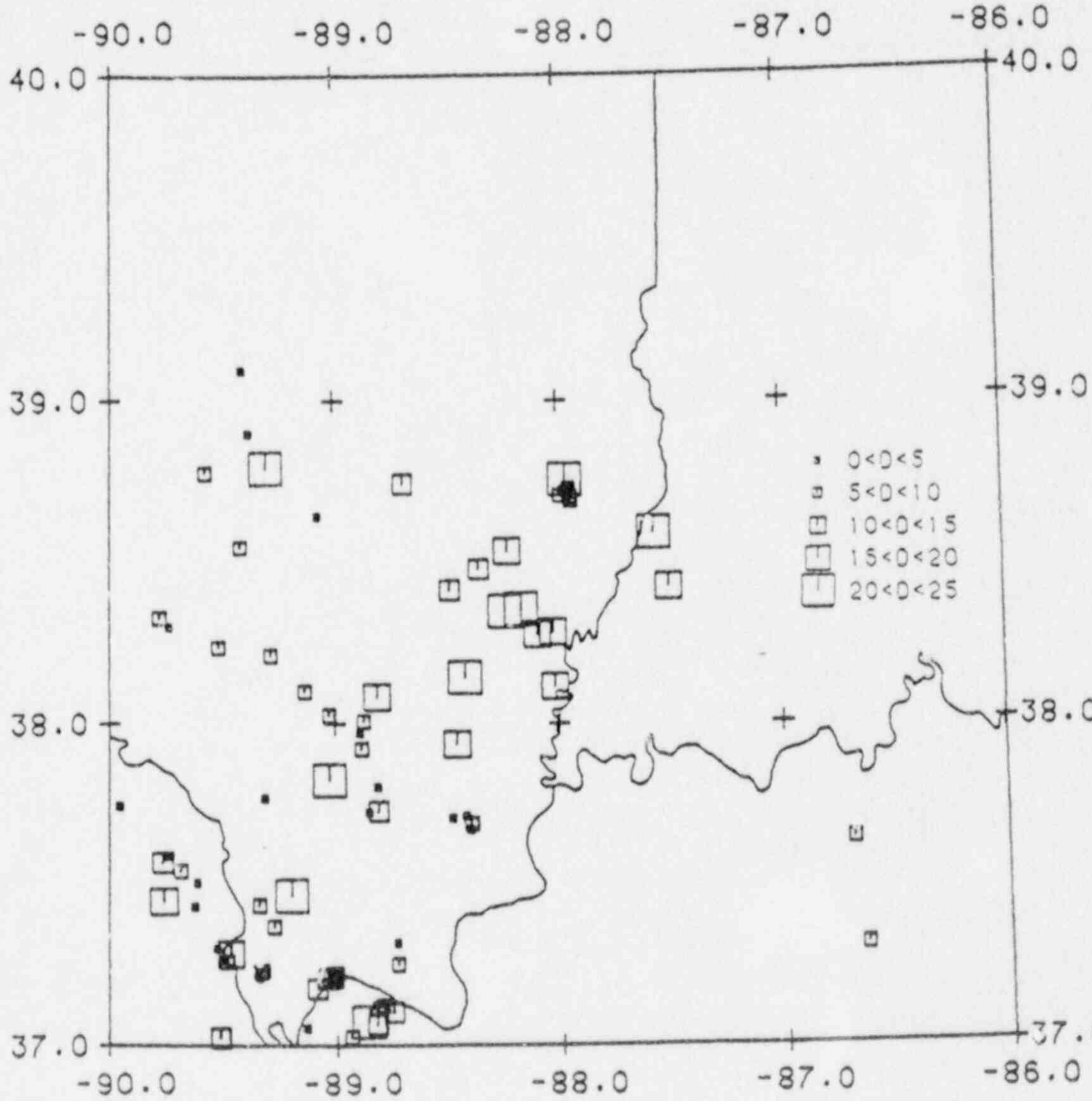

Fig. 9. Free depth instrumental locations for the time period 1974 - 1987. The symbol are keyed to the event focal depth.

ad hoc modification of the SLU network UPLANDS earth model (Stauder *et al.*, 1987) to account for the thick paleozoic sedimentary section in the source zone. The best fit mechanism is shown with the data in Figure 10. This mechanism has tension, T, and pressure, P, axes with trend 346° and plunge 17° for the T axis and trend 83° and plunge 22° for the P axis.

Surface Wave Analysis

Vertical long-period Rayleigh-wave data in the 6 to 40 second period range were obtained from 19 stations: SCH, OTT, MNT, STJ, WES, SCP, PAL, BLA, SHA, JCT, LUB, BKS, COR, NEW, PNT, SES, EDM, FFC, and YKC. range. In addition, long-period Love-wave data in the 7 to 40 second period range were available from 10 stations: STJ, WES, SCP, PAL, SHA, BKS, PNT, EDM, FFC, and YKC. The data set consisted of 225 Rayleigh-wave and 113 Love-wave spectral amplitude-period data pairs. Surface-wave focal mechanism analysis was performed using the techniques outlined by Herrmann (1979a). Because of the sensitivity of results on uncertainty in the anelastic attenuation coefficients used, spectral amplitude data were used only for stations with epicentral distances less than 3500 km.

A systematic search for the focal mechanism and seismic moment which best fit the observed spectral amplitude radiation pattern was performed. Identical searches were made over a range of focal depths between 2 and 20 kilometers. For each depth, the theoretical Rayleigh- and Love-wave radiation patterns calculated from a mechanism defined by values of strike, dip and slip angles, were compared to the observed data. The theoretical patterns were calculated using the Central U. S. earth model which is given in Herrmann (1986). A two degree increment in the slip, dip and strike angles was used in the final search.

For each mechanism, the correlation coefficient between the observed and theoretical radiation patterns, RR and RL as well as two independent seismic moment estimates, MR and ML, were computed using the independent Rayleigh and Love wave data sets, respectively. The product, RR * RL * the ratio of ML/MR or MR/ML (if ML > MR), gave an estimate of the goodness of fit for each mechanism. This product was largest for a source depth of 10 ± 1 km. Taking this product as a weighting function, a weighted average solution was obtained. Using the P-wave first motion data to specify the compressional and tensional quadrants and also to resolve the 180 degree ambiguity in nodal plane orientation, a surface-wave based solution was found. The two nodal planes are defined by the following parameters: stk= 40.6° ± 5.9°, dip= 76.2° ± 5.6, slip= 159.7° ± 6.0° for the first, and stk= 135.6° ± 5.5, dip= 70.3° ± 6.0°, slip= 14.6° ± 5.7° for the second. The corresponing tension and pressure axes have trend= 357°, plunge= 24°, and trend= 89°, plunge= 4°, respectively. The estimated seismic moment for this mechanism is 3.1×10^{23} dyne-cm.

Figure 11 shows the surface-wave solution together with the first motion data presented in Figure 10. Figure 12 shows the nodal planes corresponding to the best surface-wave solution and also the error bounds are shown. The surface-wave solution differs from the P-wave solution by requiring the N30°E striking nodal plane to dip less steeply and to the southeast. Only 4% of the P-wave first motions are inconsistent, which is not unexpected given the uncertainties in knowing the true earth model. Because of the compatibility of the surface-wave solution with the P-wave first motion data, the surface-wave solution is preferred.

To demonstrat how this solution fits the surface-wave spectral amplitude data, theoretical surface-wave radiation patterns are plotted with together with the anelastic attenuation corrected observed data in Figure 13. These patterns are scaled for a step dislocation of 3.1×10^{23} dyne-cm and are for the weighted average mechanism. One can see the 180° symmetry in both the Rayleigh- and Love-wave theoretical radiation patterns. The largest azimuthal gap in the Rayleigh-wave data is 80°, but due to this symmetry the largest actual gap in the data is 34°. For the Love-wave data the largest and largest actual gaps are 98° and 58° respectively.

Discussion

Since 1838, there have been 38 earthquakes inclusively, located within 100 km of the June 10, 1987 epicenter, with MM Intensities ≥ IV (Nuttli, 1983). Nine of these occurred during the last 30 years. Focal mechanisms, using surface-wave techniques, have been calculated for only three of

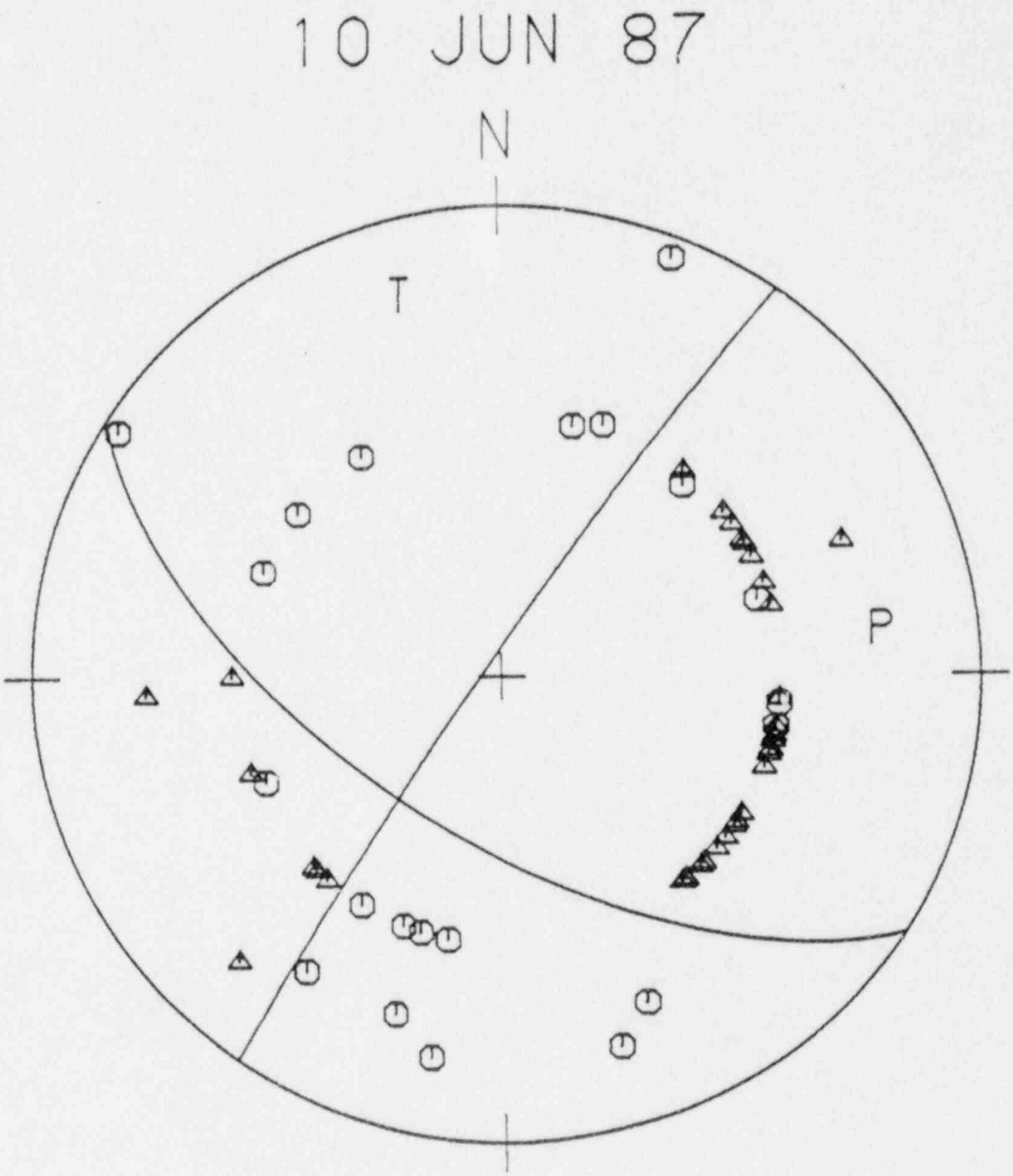

Fig. 10. P-wave focal mechanism of the 10 June 1987 earthquake.

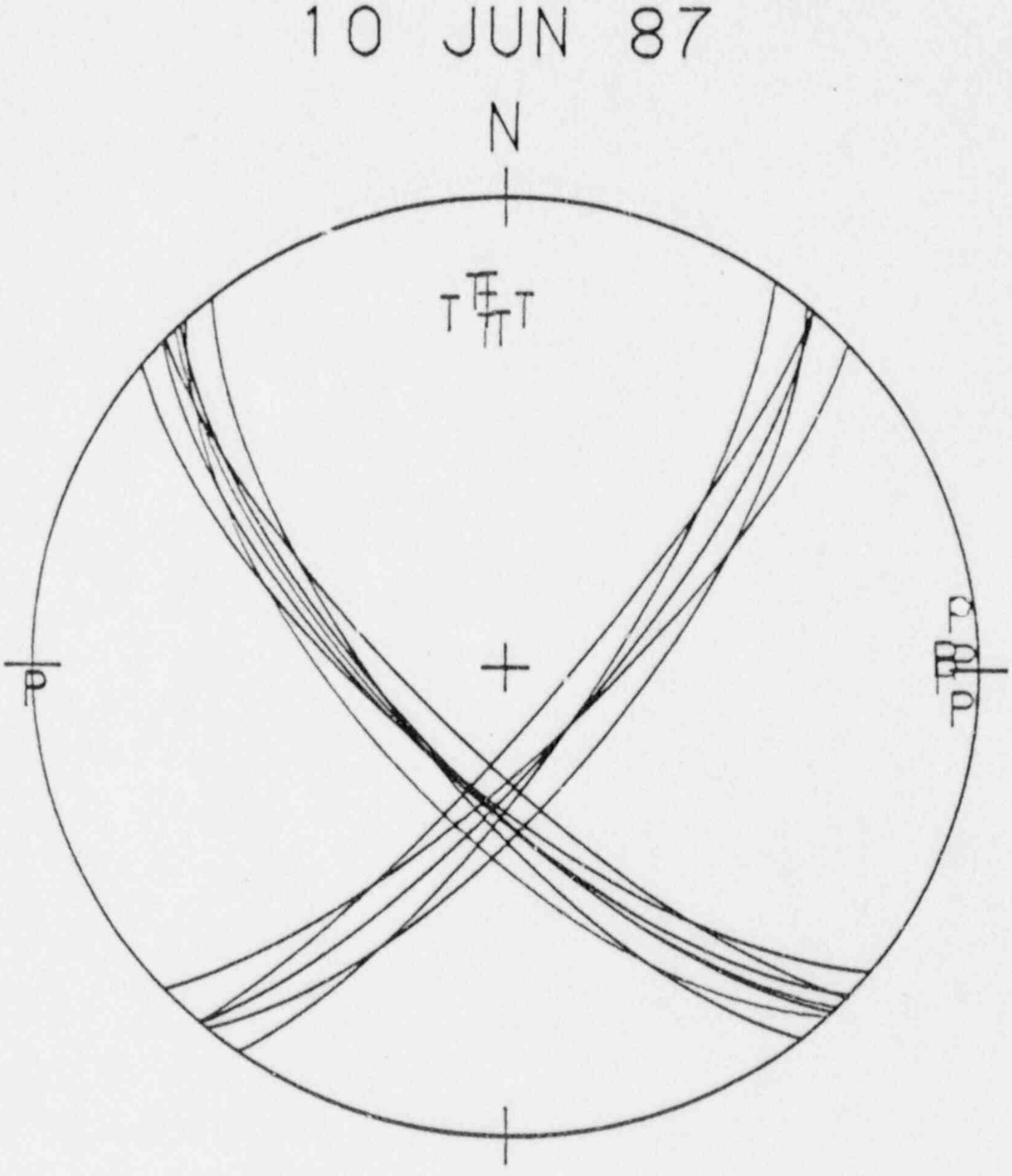

Fig. 11. Focal mechanism solution that best fits the surface-wave spectral amplitude data and the P-wave first motion data.

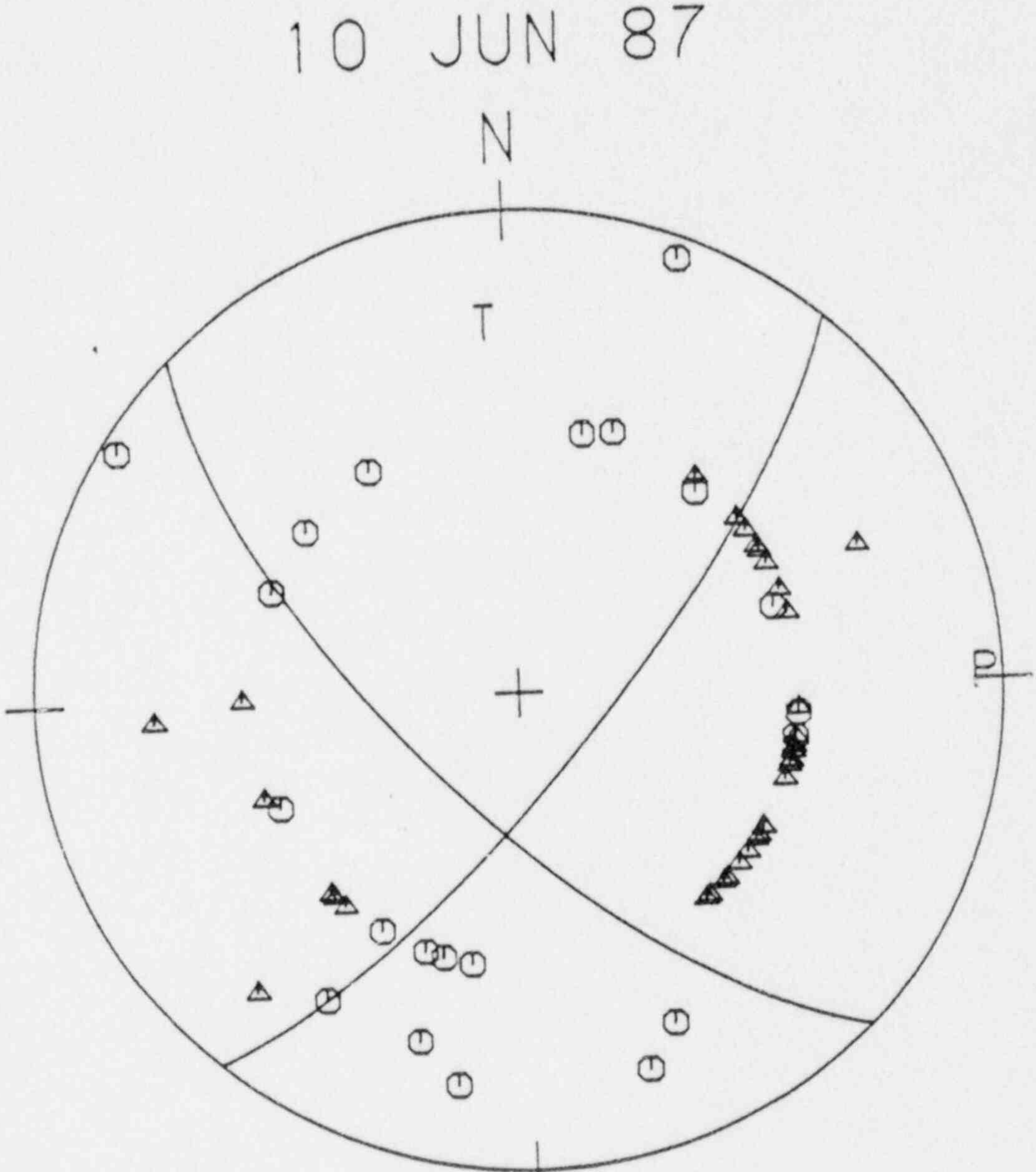

Fig. 12. Nodal planes indicating 95% confidence limits based upon the surface-wave solution. This solution agrees with all but 4% of the P-wave first motions.

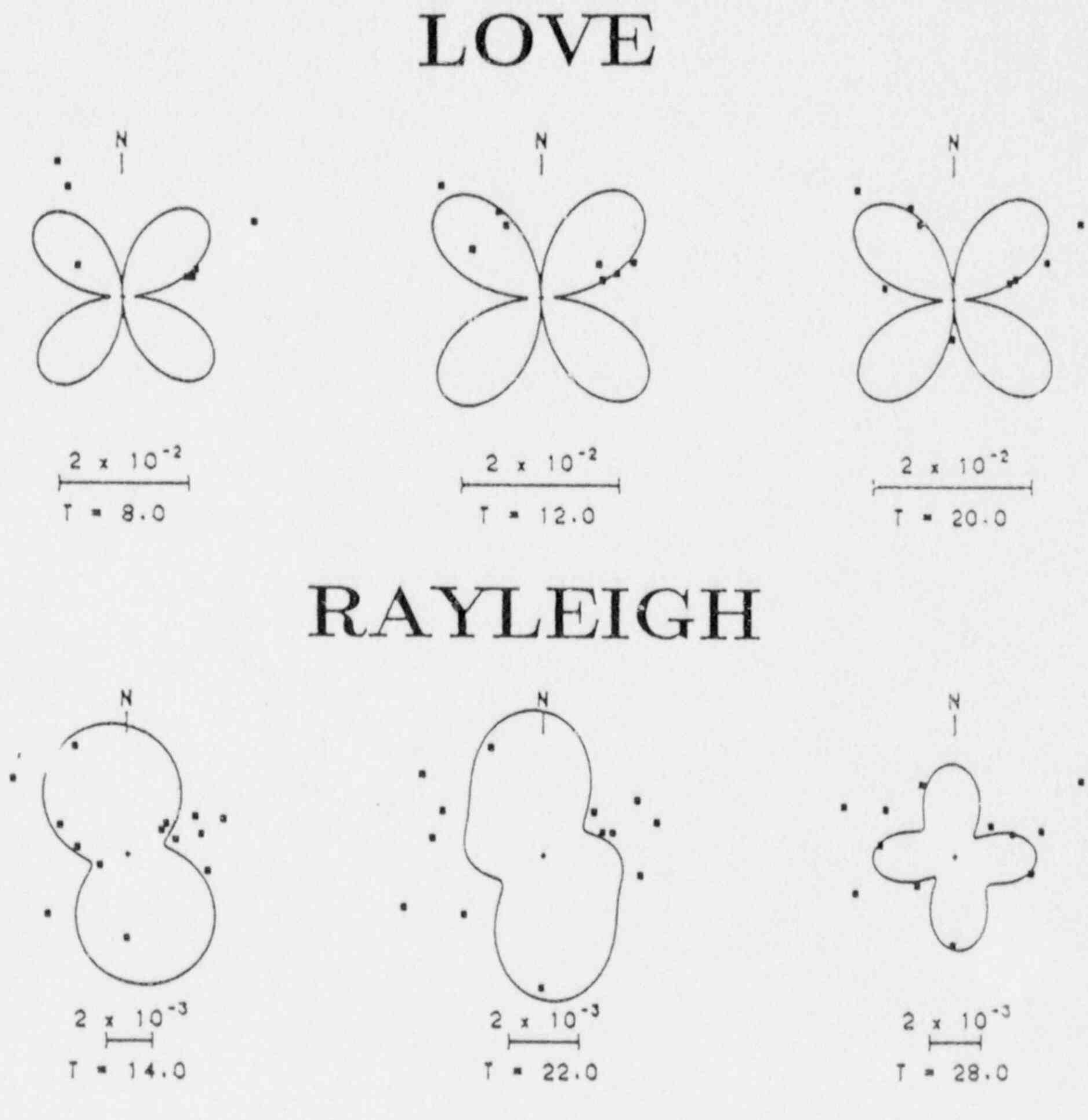

Fig. 13. Comparison of observed and predicted surface-wave radiation patterns at selected periods. The scale indicates the fundamental mode spectral amplitude in units of cm-sec at selected periods.

these events. These are listed in Table 2.

Street (1976) and Street *et al* (1974) have reported additional mechanisms in this region, obtained using P-wave first motion from first and secondary P arrivals. Herrmann and Canas (1979) argue, however, that mechanisms obtained from second-phase arrivals could have large errors because the secondary arrivals are not refracted arrivals but rather supercritically reflected, and would have undergone a phase change. For this reason, Street's mechanisms are not referenced.

Comparing the mechanisms listed in Table 2, one can see the mechanism of the June 10, 1987 main shock is very similar to one reported by Herrmann (1979), for a 3 April 1974 event located 16 km southwest of the June 10, 1987 event (Gordon, 1983). Both events are strike-slip with a small component of dip-slip. These mechanisms are in contrast with one from the 9 November 1968, $m_b = 5.5$, earthquake located 100 km to the southwest. That event is reverse dip-slip (Stauder and Nuttli, 1970; Herrmann, 1973b). All three mechanisms have pressure axes oriented east-west, but the tension axis for the November 9 event is near vertical, while the other mechanisms have tension axes nearly horizontal, in a north-south orientation.

Table 2

Source Parameters of Recent Events

Event Date	Tension Tr	Tension Pl	Pressure Tr	Pressure Pl	Depth (km)	M_o (dyne-cm)	Ref.
09 Nov 1968	192	82	97	1	22	$9.0 * 10^{23}$	1
03 Apr 1974	173	14	267	14	15	$3.7 * 10^{22}$	2
10 Jun 1987	357	23	89	5	10	$3.1 * 10^{23}$	3

1 -- Herrmann (1973)
2 -- Herrmann (1979)
3 -- Taylor and Herrmann (this study)

SOURCE PARAMETERS OF THE NORTHEASTERN OHIO EARTHQUAKE OF 31 JANUARY 1986

By Robert B. Herrmann and Bao V. Nguyen

Focal Mechanism

This earthquake occurred at 1646 UT on 31 January 1986 and was located at $41.65^\circ N$ and $81.16^\circ W$. The magnitude of this event is given as $m_{Lg} = 5.0$ (NEIC). A discussion of the location of this event in relation to other known earthquakes in the region is given by Nicholson *et al* (1988). The object of this paper is to present the surface-wave focal mechanism solution and also to address the strong motion accelerogram triggered by this event.

The focal mechanism of this earthquake was determined using the technique outlined by Herrmann (1979b). This consisted of analyzing the long period surface waves generated by this event to find a focal mechanism that best fit the surface-wave spectral amplitude data as well as the P-wave first motion data. Love-wave data were available from the following 14 seismograph stations in North America: BLA, BLO, DUG, EDM, FFC, FRB, LHC, LON, MNT, OTT, PNT, SHA, WES and YKC. Rayleigh-wave data were available from 15 stations: BLA, BLO, DUG, EDM, FFC, FRB, GOL, LHC, MNT, OTT, PNT, SCP, SHA, WES and YKC. Figure 14 shows the locations of these stations with respect to the earthquake. The spectral amplitude data were processed using multiple filter techniques and were culled according to group velocity to yield a consistent data set for source parameter determination. The final data set consisted of 234 period-amplitude pairs in the period range of 4 - 50 seconds for Love waves and 279 period-amplitude pairs in the period range of 4 - 50 seconds for Rayleigh waves.

Using the surface-wave eigenfunctions from the CUS earth model (Herrmann, 1979b), The best fit between observed and predicted surface-wave spectral amplitudes and also P-wave first motion data, was for a focal depth of 4 km, a seismic moment of $1.1\ 10^{23}$ $dyne-cm$, and a dip of 70°, a slip of 10° and a strike of 115°. For this solution, the correlation coefficients between the anelastic attenuation corrected observed and the predicted spectral amplitudes were RR = 0.881 and RL = 0.844 for the Rayleigh- and Love-wave data, respectively.

Since the surface-wave data of this earthquake were of very high quality, average Love- and Rayleigh-wave group velocities were determined. These data were inverted to determine an earth model, and eigenfunctions were computed for this new model, and the search technique repeated. This yielded a focal depth of 7 km, a seismic moment of $1.21\ 10^{23}$ $dyne-cm$, a dip of 70°, a strike of 115° and a slip of 21°. The use of slightly different earth model yielded a deeper focal depth, pointing out the problem of determining shallow focal depths from long-period surface-wave data. The focal mechanisms are essentially the same, and Both mechanisms are plotted in Figure 15 together with the P-wave first motion data. All first motion data were determined by the authors and only very sharp arrivals were used.

Figure 16 presents a comparison of the observed and predicted radiation patterns for the focal mechanism at a 7 km depth. The overall fit is quite good, as indicated by the high correlation coefficients.

Because the P-wave first motion data are very good, there is little doubt that the correct focal mechanism has been found. The use of a surface-wave spectral amplitude data by itself leads to a certain ambiguity, since the spectral amplitude data have no information to resolve the compressional and dilatational quadrants. In addition, the surface-wave spectral amplitude data are invariant to a 180° rotation of the nodal plane. Figure 17 compares observed and synthetic seismograms for the 7km solution at the station WES, a distance of 833 km from the earthquake. All seismograms start 197.6 seconds after the origin. The vertical component traces are plotted in the left column, and the transverse traces in the right. Traces (a) and (d) are the observed traces, and the others are synthetics. (b) and (c) are for the preferred focal mechanism shown in Figure 14. The agreement in shape, polarity and amplitude is good. (c) and (f) present the seismograms obtained by rotating the mechanism by 180°. The Love wave seismogram does not change much,

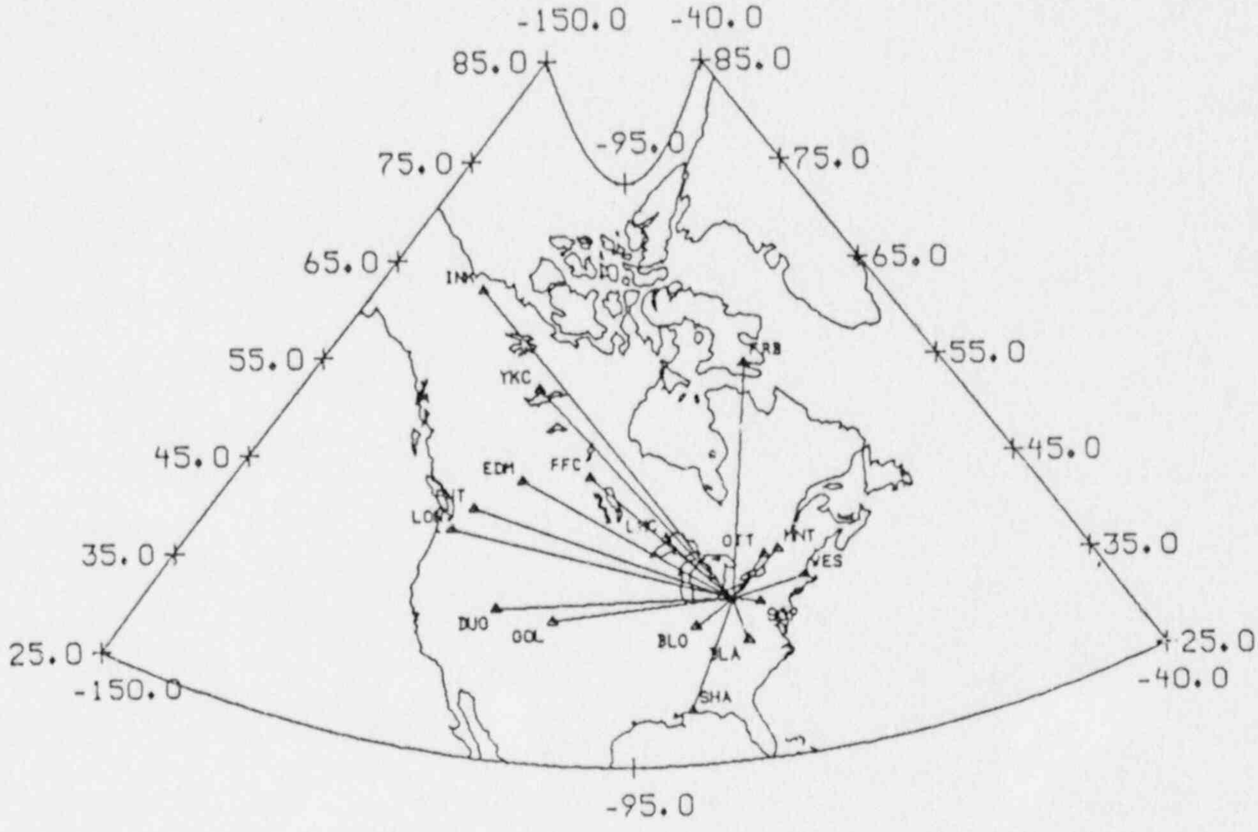

Fig. 14. Distribution of seismograph stations providing long period surface-wave data for the northeastern Ohio earthquake of January 31, 1986.

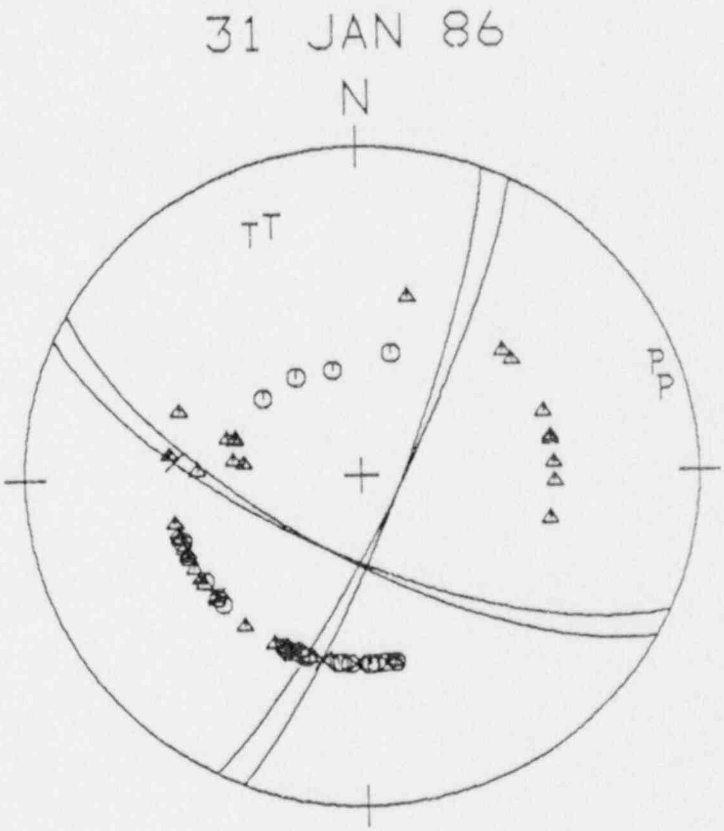

Fig. 15. Focal mechanism plots for the 4 and 7 km deep solutions. Compressional P-wave first motions are indicated by the octagons, dilatations by triangles and uncertain low amplitude arrivals by the 27's.

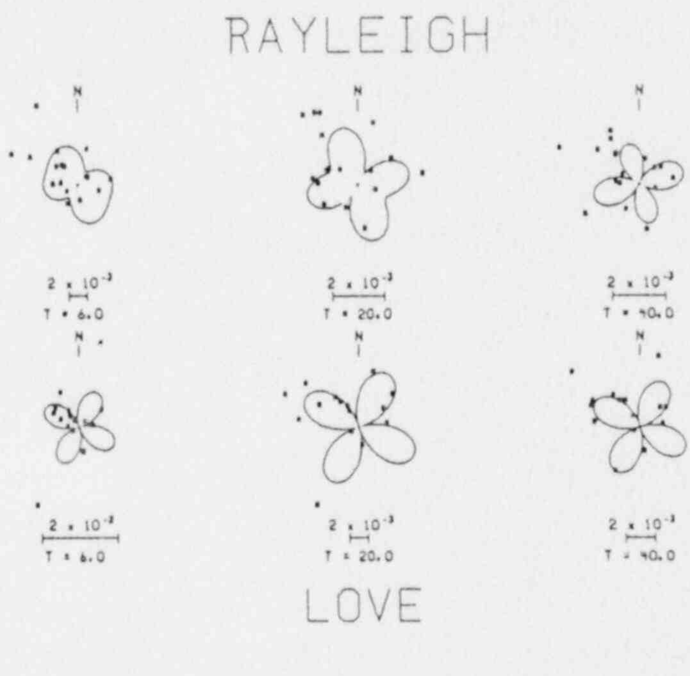

Fig. 16. Comparison of observed and predicted surface-wave radiation patterns. All spectral amplitudes have been corrected for anelastic attenuation back to the source. The corrected spectra are presented at a reference distance of 1000 km. The scaling bars indicate the spectral amplitudes in units of *cm-sec*.

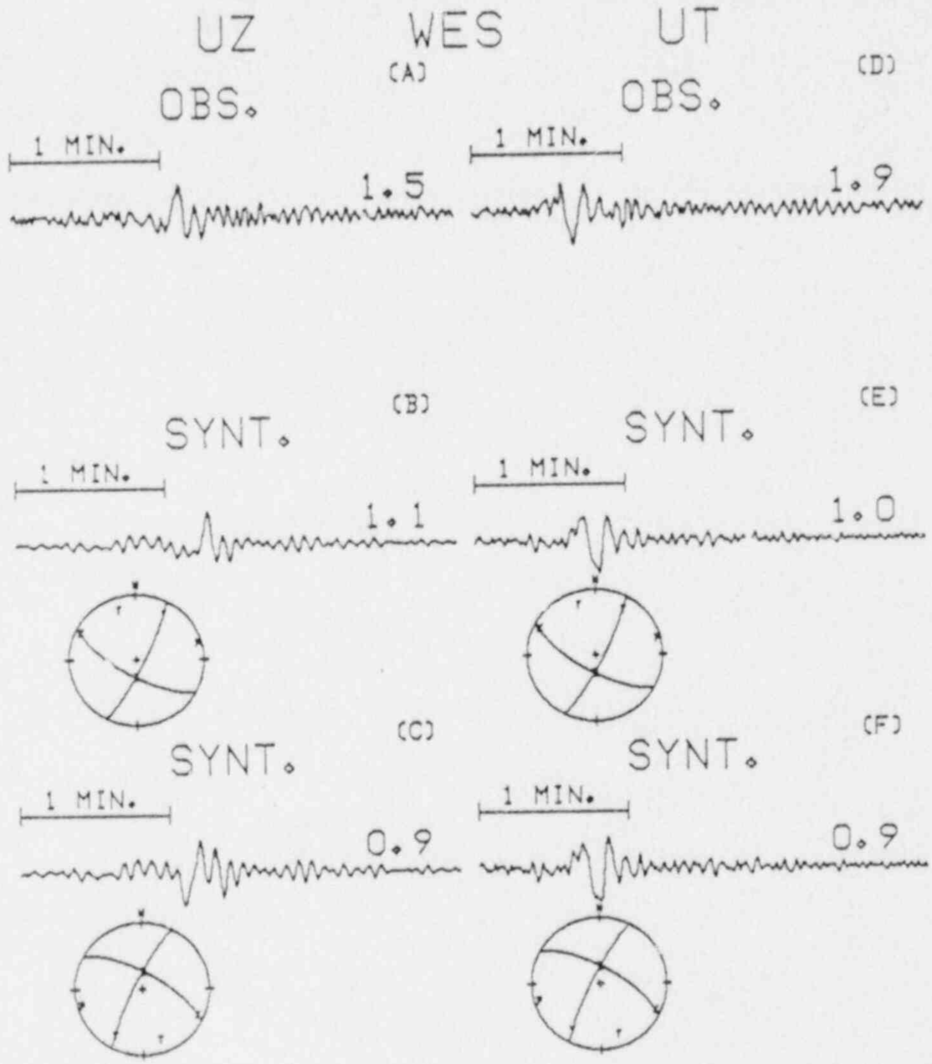

Fig. 17. Comparison of observed and predicted seismograms at WES, 833 km from the earthquake. The numbers represent peak amplitudes on a WWSSN long-period seismogram with a gain of 3000.

but there is a difference in the vertical component seismograms. The interchange of P and T axes would invert the predicted waveforms, and is clearly not acceptable. This comparison supports the focal mechanism solution chosen.

Strong Motion Accelerogram

This earthquake triggered strong motion instruments at a site approximately 16 km due north (Wesson and Nicholson, 1986). The presence of these data provides an opportunity to address a number of interesting questions. First, this data set can be used to provide an independent check on the surface-wave focal mechanism solution. It can also provide some information on the duration of the source time function, which addresses the issue of earthquake source spectrum scaling. Finally, the ability of modeling the ground motion time histories can be tested.

The major assumptions in modeling a seismic time history are that the source and earth structure are known and also that the observed time history is without error. In the absence of this knowledge, one must iteratively construct a reasonable model.

The first shallow earth model used was based on one Herrmann (1969) obtained for southern Ohio, through the use of short period Rayleigh-wave dispersion. This model, HER, is given in Table 3. The model consists of two layers over a halfspace, with equal layer thicknesses for the layers. The overall thickness of the sedimentary section of 2.0 km was chosen to match the depth to Precambrian near the epicenter. Figure 18 compares the observed and predicted velocity time histories. In all plots to follow the top trace is the velocity time history from the integrated accelerogram at the foundation of the Perry NPP. The units are ground velocity in cm/sec. The purpose of the time history comparisons is to see if the data can be fit, to see if the focal mechanism is correct, and to estimate the duration of the source time function. Figure 18 has a source pulse with a duration of 0.5 seconds, and a focal mechanism with strike of $115°$, slip of $10°$, and a dip of $70°$. A seismic moment of $1.0\ 10^{23}\ dyne-cm$ as well as an epicentral distance of 16 km are used for all figures. This figure compares the observed time histories (a) with synthetics for focal depths of 3 km (b), 4 km (c), 6 km (d) and 8 km (e). The shallow focal depths are rejected because of the strong secondary arrivals in the synthetics which are not seen in the observed waveforms. The shallow events are setting up a strong reflection in the layers at this distance. One guide used to judge the goodness of fit is the relative amplitudes among the various components. For example, the observed peak velocites are roughly (1.7, 1.8, 2.2) for the (Z, N, E) components. The synthetics generally have $N \tilde{} E$, but $Z << N$. The peak Z motion is not well modeled. As will be seen, this is a characteristic of all models.

Figure 19 shows the effect of rotating the focal mechanism by $180°$. Recall that the surface-wave spectral amplitude data are invariant to such a change in focal mechanism. At short distances, a major change is seen in the waveforms. Now the predicted time histories have $Z \tilde{} N$ and $Z,N << E$, which is drastically at odds with the observations.

Figures 20-23 provide a complete set of time histories that compare the effects of the duration of the source time function and the focal depth. In each of these figures, the focal mechanism is held fixed at the values used for Figure 18, traces (b) , (c), (d), (e), and (f) represent source time function durations of 0.1, 0.2, 0.3, 0.4 and 0.5 seconds, respectively. Figures 20, 21, 22 and 23 are for focal depths of 3.0, 4.0, 6.0 and 8.0 km. The best fit to the E component (SH wave) occurs for depths of 6.0 and 8.0 km and source time functions with total duration of 0.3 and 0.4 seconds. The peak amplitudes of the N and E components are matched well with the seismic moment used for the source time function duration of 0.3 seconds. The amplitude of the vertical component time history is underestimated by a factor of 2-3.

The report by Wesson and Nicholson (1986) emphasizes the presence of 20 meters of glacial till near the strong motion instrument site. The model OHER was modified by adding 18 meters of low velocity material near the surface, the HER1 model of Table 3. The time histories generated for the same mechanism, a focal depth of 6.0 km, and the $1.0\ 10^{23}\ dyne-cm$ seismic moment are shown in Figure 24. In this figure, (b) through (f) represent changes in the source pulse duration from 0.1 to 0.5 seconds in increments of 0.1 seconds. Comparing this figure to Figure 22, the simple model at the same depth, shows the effect of the till layer. For a given source pulse duration,

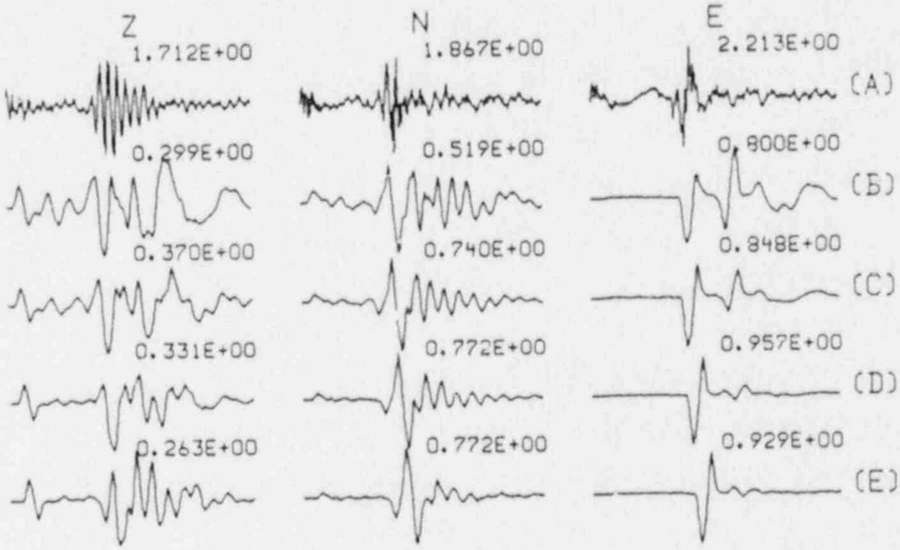

Fig. 18. Comparison of observed and synthetic time histories for the strong motion site using the model OHER. Velocity time histories are plotted (cm/s). Z is positive up, N is positive to the north and E is positive to the east. (a) are the observed, unfiltered ground velocities. The synthetics are for a seismic moment of 1.0 10^{23} dyne-cm, a strike of 120°, a dip of 70°, and a slip of 10°. The source time function has a duration of 0.5 seconds. (b) focal depth of 3 km. (c) focal depth of 4 km. (d) a focal depth of 6 km. (e) a focal depth of 8

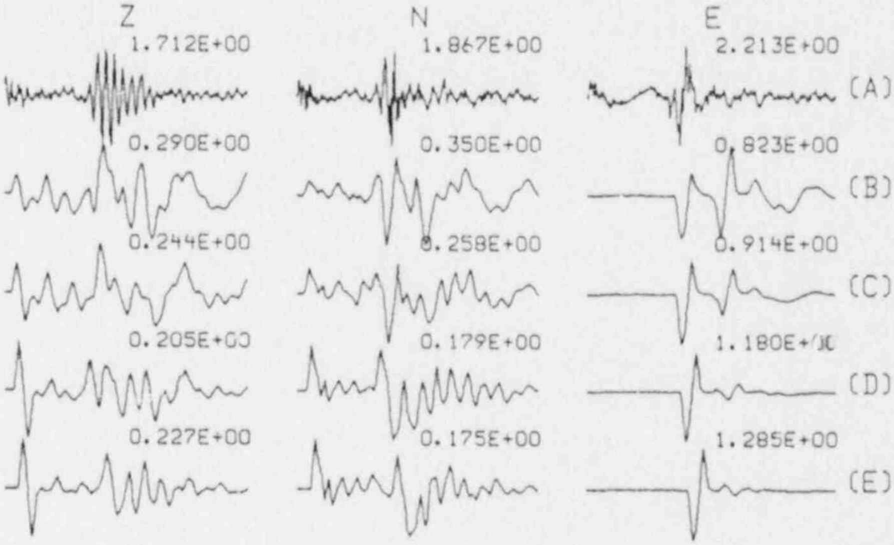

Fig. 19. Comparison of time histories as a function of focal depth using the model OHER. This focal mechanism differs in that the strike is 300°.

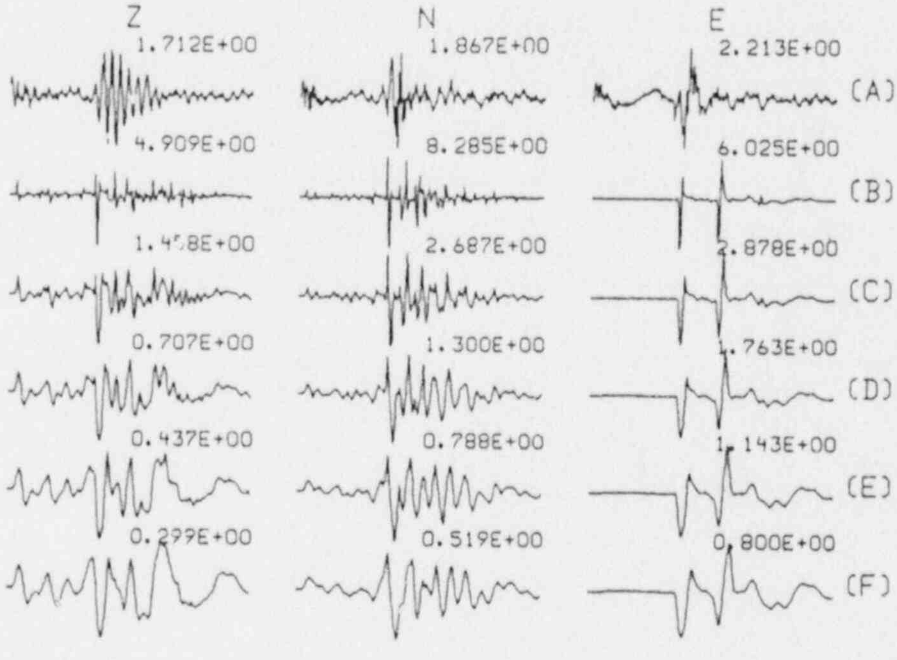

Fig. 20. Comparison of observed and synthetic time histories using the model OHER. (a) are the observed, unfiltered ground velocities. The synthetics are for a seismic moment of 1.0 10^{23} dyne-cm, a strike of 120°, a dip of 70°, and a slip of 10°. The focal depth is 3 km. the source pulse durations are (b) 0.1 sec, (c) 0.2 sec, (d) 0.3 sec, (e) 0.4 sec, and (f) 0.5 sec.

Fig. 21. Comparison of observed and synthetic time histories using the model OHER. (a) are the observed, unfiltered ground velocities. The synthetics are for a seismic moment of 1.0 10^{23} dyne-cm, a strike of 120°, a dip of 70°, and a slip of 10°. The focal depth is 4 km. the source pulse durations are (b) 0.1 sec, (c) 0.2 sec, (d) 0.3 sec, (e) 0.4 sec, and (f) 0.5 sec.

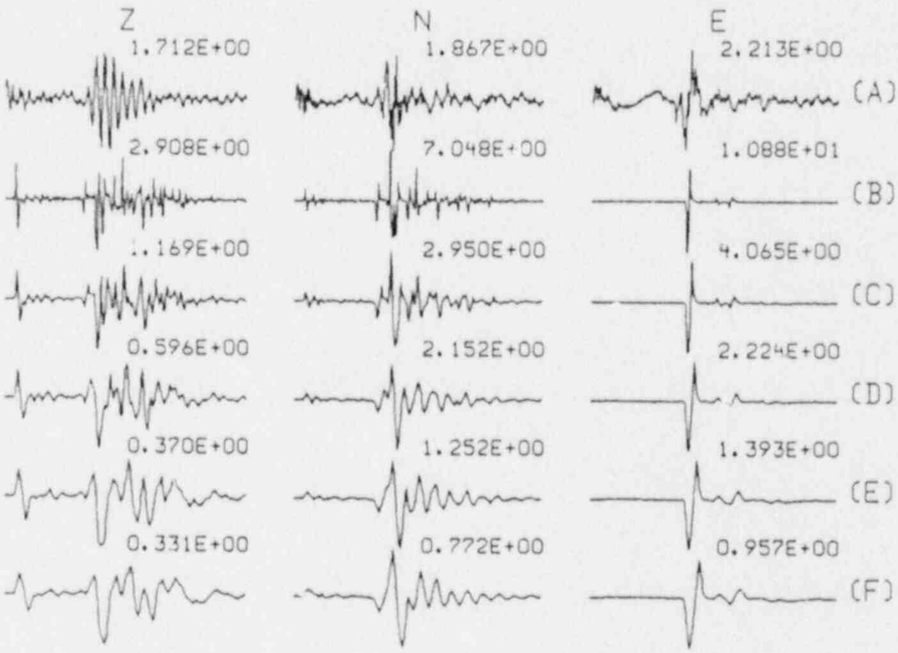

Fig. 22. Comparison of observed and synthetic time histories using the model OHER. (a) are the observed, unfiltered ground velocities. The synthetics are for a seismic moment of 1.0 10^{23} dyne-cm, a strike of 120°, a dip of 70°, and a slip of 10°. The focal depth is 6 km. the source pulse durations are (b) 0.1 sec, (c) 0.2 sec, (d) 0.3 sec, (e) 0.4 sec, and (f) 0.5 sec.

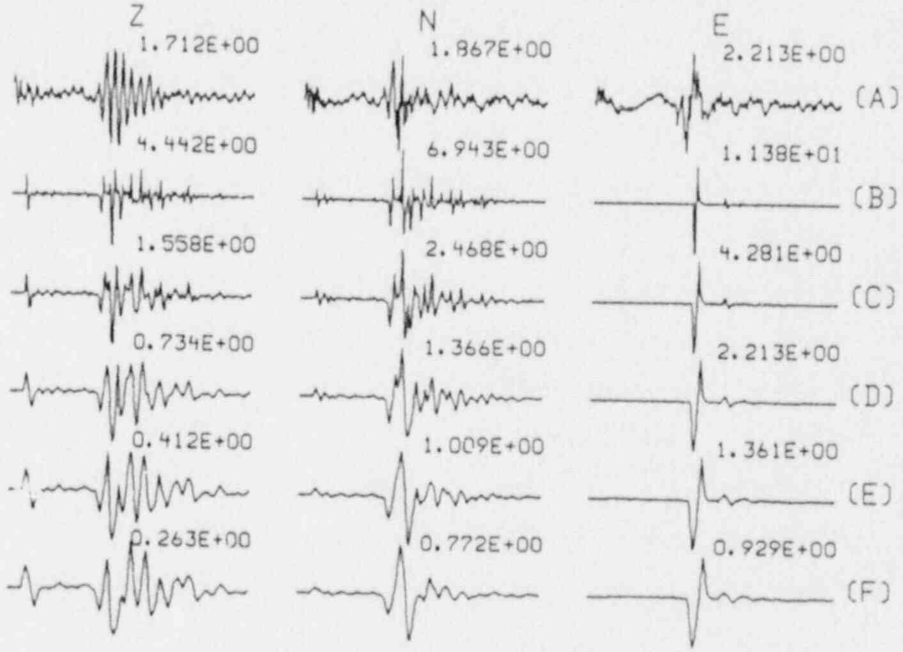

Fig. 23. Comparison of observed and synthetic time histories using the model OHER. (a) are the observed, unfiltered ground velocities. The synthetics are for a seismic moment of 1.0 10^{23} dyne-cm, a strike of 120°, a dip of 70°, and a slip of 10°. The focal depth is 8 km. the source pulse durations are (b) 0.1 sec, (c) 0.2 sec, (d) 0.3 sec, (e) 0.4 sec, and (f) 0.5 sec.

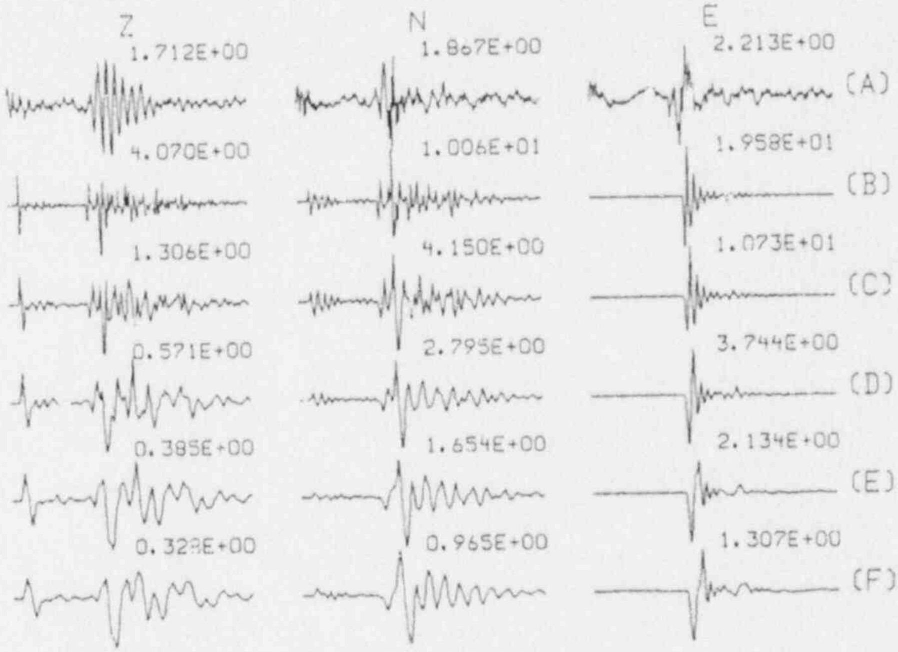

Fig. 24. Comparison of observed and synthetic time histories using the model OHER1. (a) are the observed, unfiltered ground velocities. The synthetics are for a seismic moment of 1.0 10^{23} dyne-cm, a strike of 120°, a dip of 70°, and a slip of 10°. The focal depth is 6 km. the source pulse durations are (b) 0.1 sec, (c) 0.2 sec, (d) 0.3 sec, (e) 0.4 sec, and (f) 0.5 sec.

the free surface amplitudes are increased by factors between 1 and 2, with the shorter pulses yielding the greater increases. The waveforms have also changed, with the presence of reverberations following the initial pulse. The 0.2 second pulse (c) gives a good match to shapes, but the amplitudes are too high compared to the observed.

The inability of modeling the vertical component motion, led to the use of other models. Detailed site specific investigations were made at the Perry NPP that are given in the PSAR (Cleveland Electric Illuminating Company, (1974). Examining this, Figure 25 was generated using the model PER5. This model has the 18 m glacial till layer at the surface, and a different model for the next two km than that used above. There is still a problem with the predicted vertical components. Finally, the effect of more detailed structure in the till was examined with model PER10, Figure 26. In addition the lower structure differs from that of model PER5 by the presence of a layer boundaries at 380, 850 and 1800 meters instead of 400, 1000 and 2000 meters. For a source pulse with duration of 0.3 seconds (d), model PER10 gives a nice waveform fit to the N component, but again underestimates the Z component.

The examples given here show the dependence of the predicted time histories upon the earth model used. Data from a single station cannot be used to define all parameters of the model, focal mechanism and source time function. A source time function with a duration of 0.3 seconds and the surface-wave seismic moment does not do too poorly in fitting the N and T time histories. The Z time history has not been fit. On the basis of this effort, one might question the quality of the Z component accelerogram. Following the earthquake, the USGS emplaced digital GEOS instruments to record aftershocks (Borcherdt, 1986). One of these instruments, designated as station 001 was located near the strong motion instrument site. Recorded aftershocks usually show that the S-wave on the vertical component is smaller than that on the horizontal components, as the above synthetics would require. However, a recording of the event at 19:47 on February 3, 1986 showed a vertical component S-wave time history the same size as the horizontal recordings of the same arrival. Thus the high motion on the vertical accelerogram cannot be discounted and requires modeling.

To do this modeling much more is required to be known about the earth model and about the aftershock sequence. The digital instruments recorded surface waves from a nearby quarry. Other seismographs in the area are recording surface waves from strip mining operations in the state. These data can be used to refine the shear-wave velocity model in the upper 2 km of the section. The aftershock data could then be used to refine the velocity model by attempting to model the seismic waveforms. Finally, a second attempt could be made to understand the strong motion accelerogram.

Conclusions

The source parameters of the 31 January 1986 earthquake were obtained from an analysis of long-period surface waves and P-wave first motion data. An attempt was made to test this solution by modeling a strong motion recording of the earthquake. In general, the surface-wave solution is adequate, but shorter duration source pulses may require a smaller seismic moment, especially if low-velocity sediments are placed at the surface.

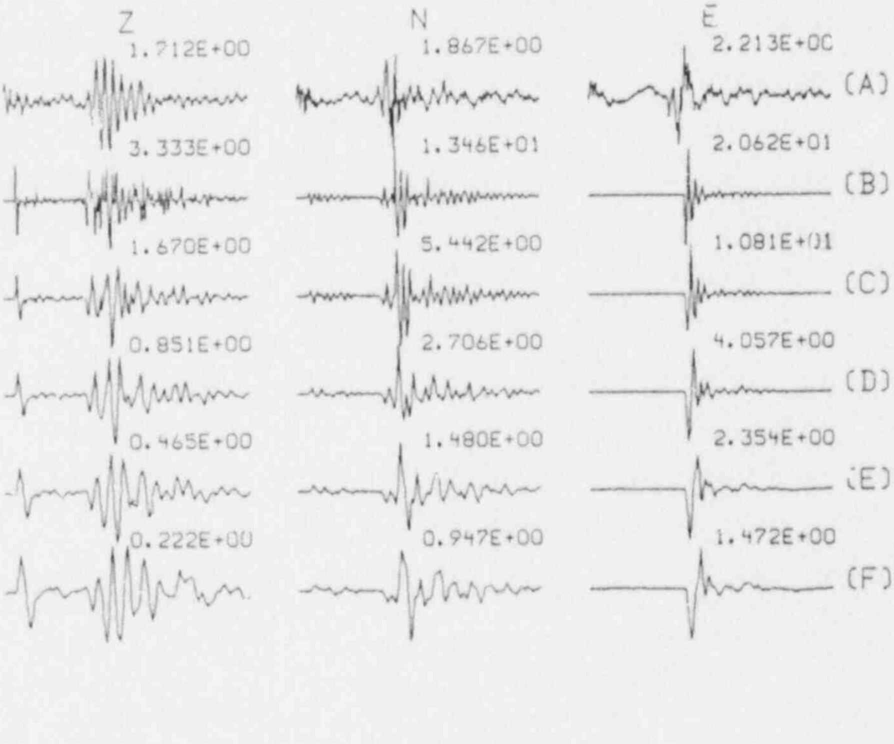

Fig. 25. Comparison of observed and synthetic time histories using the model PER5. (a) are the observed, unfiltered ground velocities. The synthetics are for a seismic moment of 1.0 10^{23} dyne-cm, a strike of 120°, a dip of 70°, and a slip of 10°. The focal depth is 6 km. the source pulse durations are (b) 0.1 sec, (c) 0.2 sec, (d) 0.3 sec, (e) 0.4 sec, and (f) 0.5 sec.

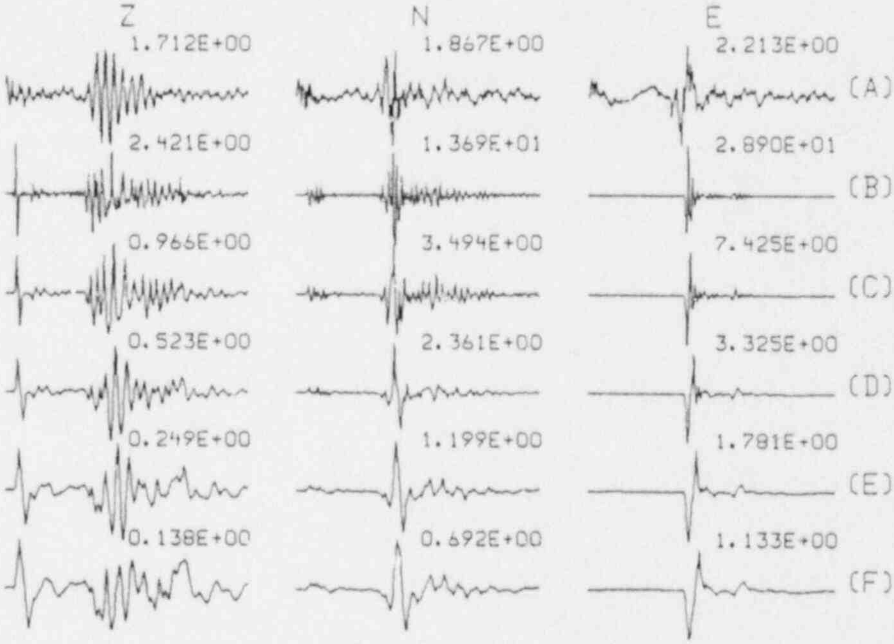

Fig. 26. Comparison of observed and synthetic time histories using the model PER10. (a) are the observed, unfiltered ground velocities. The synthetics are for a seismic moment of 1.0 10^{23} dyne-cm, a strike of 120°, a dip of 70°, and a slip of 10°. The focal depth is 6 km. the source pulse durations are (b) 0.1 sec, (c) 0.2 sec, (d) 0.3 sec, (e) 0.4 sec, and (f) 0.5 sec.

Table 3.
Earth Models for Synthetic Seismograms

H (km)	P-Vel (km/s)	S-Vel (km/s)	Density (gm/cc)	Qa	Qb
HER Model					
1.0	3.70	2.14	2.20	0.0025	0.0050
1.0	5.60	3.23	2.70	0.0025	0.0050
	6.33	3.60	2.80	0.0025	0.0050
HER1					
.018 1.525	0.40	1.50	0.0500	0.0500	
1.0	3.70	2.14	2.20	0.0025	0.0050
1.0	5.60	3.23	2.70	0.0025	0.0050
	6.33	3.60	2.80	0.0025	0.0050
PER5 Model					
.018	1.525	0.40	1.50	0.0500	0.0500
0.4	3.00	1.58	2.00	0.0050	0.0100
0.6	3.70	2.14	2.20	0.0025	0.0050
1.0	5.60	3.23	2.70	0.0025	0.0050
	6.33	3.60	2.80	0.0025	0.0050
PER10 Model					
.002	0.365	0.182	1.96	0.0500	0.0500
.002	1.524	0.213	1.96	0.0500	0.0500
.003	1.524	0.365	2.07	0.0500	0.0500
.004	1.798	0.579	2.11	0.0500	0.0500
.007	2.377	0.792	2.26	0.0500	0.0500
.365	3.170	1.493	2.77	0.0050	0.0100
0.50	3.70	2.29	2.50	0.0025	0.0050
1.00	5.60	3.14	2.70	0.0025	0.0050
	6.33	3.60	2.80	0.0025	0.0050

LESSONS LEARNED

The NRC regional seismic networks have contributed much needed information concerning the earthquake process in the central United States. In addition to the very pronounced seismicity pattern near New Madrid, other patterns are emerging 100 km west of New Madrid on a northeast-southwest line, roughly connecting St. Louis with Little Rock. Patterns are also being seen in southern Illinois because of the existence of the NRC Wabash Valley network. The regional network data can be further used to obtain focal mechanisms for these regi s that may assist in further definition of the active source zones.

The June 10, 1987 earthquake was significant because of its size, the largest in the region since 1968. Many aftershocks were recorded in a cooperative acquisition effort by the USGS, Memphis State University, Saint Louis University, Indiana University and the University of Kentucky. The success of aftershock monitoring depends strongly upon having a very good location for the main event, which was available because of the existence of the NRC network. On the other hand, the regional network could not provide information on the ground motions generated by this earthquake because of its limited dynamic range and single component recording.

The attempts to study the larger earthquakes have made use of available data. Little is directly known about strong ground motion generation by earthquakes in the central United States, primarily because of the lack of data and the lack of high quality data. In order to be able to estimate ground motions for safety analysis, it it e ntial that the effects of the source, the site and the intervening earth structure be well understood. This can only be done by studying individual earthquakes using high quality data.

REFERENCES

Barstow, N. L., K. G. Brill, Jr., O. W. Nuttli, and P. W. Pomeroy (1981). An approach to seismic zonation for siting nuclear electric power generating facilities in the eastern United States, U. S. Nuclear Regulatory Commission NUREG/CR-1577, Washington, D. C.,

Borcherdt, R. D. (ed)(1986). Preliminary report on aftershock sequence for earthquake of January 31, 1986 near Painesville, Ohio, *U. S. G. S. Open-File Report 86-181.*

Cleveland Electric Illuminating Company (1974). Perry Nuclear power Plant Units 1 & 2, Preliminary Safety Analysis Report, Volume 3., Cleveland, Ohio.

Gordon, D. W. (1983). Revised hypocenters and correlation of seismicity and tectonics in the Central United States, Ph. D. Dissertation, Saint Louis University, 199pp.

Herrmann, R. B. (1969). The structure of the Cincinnati Arch as determined by short period Rayleigh waves, *Bull. Seism. Soc. Am.* **59**, 399-407.

Herrmann, R. B. (1973b). Surface-wave generation by the south central Illinois earthquake of November 9, 1968, *Bull. Seism. Soc. Am.* **63**, 2121-2134.

Herrmann, R. B. (1979a). FASTHYPO - A hypocenter location program, *Earthquake Notes* **52**, 25-38.

Herrmann, R. B. (1979b). Surface wave focal mechanisms for eastern North American earthquakes with tectonic implications, *J. Geophy. Res* **84**, 3543-3552.

Herrmann, R. B. (1986). Surface-wave studies of some South Carolina earthquakes, *Bull. Seism. Soc. Am.* **76**, 111-121.

Herrmann, R. B., J.-A. Canas (1978). Focal mechanism studies in the New Madrid seismic zone, *Bull. Seism. Soc. Am.* **68**, 1095-1102.

Nicholson, C., E. Roeloffs, and R. L. Wesson (1988). The northeastern Ohio earthquake of 31 January 1986: Was it induced?, *Bull. Seism. Soc. Am.* **78**, 188-217.

Nuttli, O. (1983). *Catalog of Central United States Earthquakes Since 1800 of* $m_b \geq 3.0$, St. Louis University, St. Louis, MO.

Stauder, W., R. Herrmann, C. O'Sullivan, S. Neiers, L.-J. Li, C.-F. Shieh, B. Nguyen, S. Horton, K. Taylor, J. Batllo (1987). *Central Mississippi Valley Earthquake Bulletin -- Second Quarter 1987* **52**, St. Louis University, St. Louis, MO.

Stauder, W., O. Nuttli (1970). Seismic studies: south central Illinois earthquake of November 9, 1968, *Bull. Seism. Soc. Am.* **60**, 973-981.

Street, R. (1976). Contemporary earthquake mechanisms in the central United States, *Ph.D. Dissertation*, St. Louis University, St. Louis, MO.

Street, R., R. B. Herrmann, O. W. Nuttli (1974). Earthquake mechanics in Central United States, *Science* **184**, 1285-1286.

Wesson, R. L. and C. Nicholson (eds) (1986). Studies of the January 31, 1986 northeastern Ohio earthquake, *U. S. G. S. Open-File Report 86-331.*

NRC FORM 335 (2-84) NRCM 1102, 3201, 3202

U.S. NUCLEAR REGULATORY COMMISSION

BIBLIOGRAPHIC DATA SHEET

SEE INSTRUCTIONS ON THE REVERSE

1. REPORT NUMBER (Assigned by TIDC, add Vol. No., if any)
NUREG/CR-5165

2. TITLE AND SUBTITLE
Seismological Investigation of Earthquakes in the New Madrid Seismic Zone and the Northeastern Extent of the New Madrid Seismic Zone Final Report, September 1981 - December 1986

3. LEAVE BLANK

4. DATE REPORT COMPLETED
MONTH: May YEAR: 1988

5. AUTHOR(S)
R. B. Herrmann, K. Taylor, B. Nguyen

6. DATE REPORT ISSUED
MONTH: July YEAR: 1988

7. PERFORMING ORGANIZATION NAME AND MAILING ADDRESS (Include Zip Code)
Department of Earth and Atmospheric Sciences
Saint Louis University
3507 Laclede Avenue
Saint Louis, MO 63103

8. PROJECT/TASK/WORK UNIT NUMBER

9. FIN OR GRANT NUMBER
D1694

10. SPONSORING ORGANIZATION NAME AND MAILING ADDRESS (Include Zip Code)
Division of Engineering
Office of Nuclear Regulatory Research
U.S. Nuclear Regulatory Commission
Washington, DC 20555

11a. TYPE OF REPORT
Technical

b. PERIOD COVERED (Inclusive dates)
September 1981 - December 1986

12. SUPPLEMENTARY NOTES

13. ABSTRACT (200 words or less)

Earthquake activity in the Central Mississippi Valley has been monitored by a seismograph network of eight stations in the Wabash River Valley and six stations in the New Madrid seismic zone. This network is a component of a larger network jointly sponsored by the NRC, USGS, universities and states. From October 1981 to December 1986 1206 earthquakes were located, of which 808 were in the New Madrid, Missouri area.

Focal mechanisms have been calculated for the June 10, 1987 southern Illinois earthquake using both P-wave first motions and long-period surface-wave spectral amplitude data. The solution which best fit the surface wave data together with the P-wave first motion data is one with a focal depth of 10±1 km, a seismic moment of 3.1×10^{23} dyne-cm, and a focal mechanism characterized by a pressure axis that trends 89° and plunges 4° and a tension axis that trends 357° and plunges 24°.

The long-period surface-wave and strong ground motion accelerogram recordings of the January 31, 1986 northeastern Ohio earthquake were used to estimate the focal mechanism and source time function of the source. The surface-wave solution requires a source with a depth of 7 km, a seismic moment of 1.1×10^{23} dyne-cm, and a focal mechanism characterized by a pressure axis that trends 336° and plunges 21° and a tension axis that trends 70° and plunges 7°.

14. DOCUMENT ANALYSIS - a. KEYWORDS/DESCRIPTORS
Seismicity
Central Mississippi Valley
New Madrid Seismic Zone
Focal Mechanisms

b. IDENTIFIERS/OPEN-ENDED TERMS

15. AVAILABILITY STATEMENT
Unlimited

16. SECURITY CLASSIFICATION
(This page) Unclassified
(This report) Unclassified

17. NUMBER OF PAGES

18. PRICE

*U.S. GOVERNMENT PRINTING OFFICE:1988-202-292:80127

UNITED STATES
NUCLEAR REGULATORY COMMISSION
WASHINGTON, D.C. 20555

OFFICIAL BUSINESS
PENALTY FOR PRIVATE USE, $300

SPECIAL FOURTH-CLASS RATE
POSTAGE & FEES PAID
USNRC
PERMIT No. G-67

120555078877 1 1AN1RA
US NRC-OARM-ADM
DIV OF PUB SVCS
POLICY & PUB MGT BR-PDR NUREG
W-537
WASHINGTON DC 20555

NUREG/CR-5165

SEISMOLOGICAL INVESTIGATION OF EARTHQUAKES IN THE NEW MADRID SEISMIC ZONE AND THE NORTHEASTERN EXTENT OF THE NEW MADRID SEISMIC ZONE

JULY 1988